Fragment size distributions in brittle deformed rocks.

Alison Ord[1], Thomas Blenkinsop[2] and Bruce Hobbs[1,3]

1. *School of Earth and Environment, University of Western Australia, 35 Stirling Highway, Crawley, Perth WA 6009, Australia*
2. *School of Earth and Environmental Sciences, Cardiff University, Cardiff CF10 3AT, Wales, UK*
3. *CSIRO Earth Science and Resource Engineering, PO Box 1130, Bentley, WA 6102, Australia*

Cataclasite fragment size distributions are analysed with untruncated data.

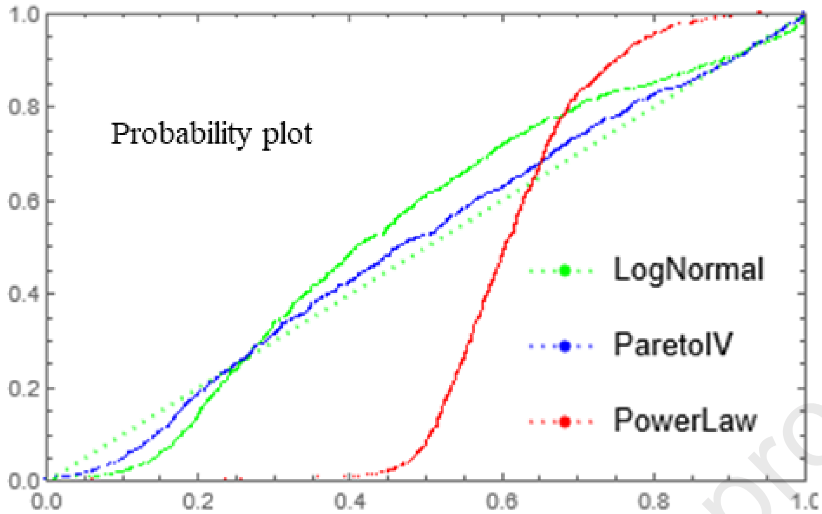

Best-fit Generalised Pareto distribution is consistent with theory.

Power-law and log-normal distributions tend to be less good fits.

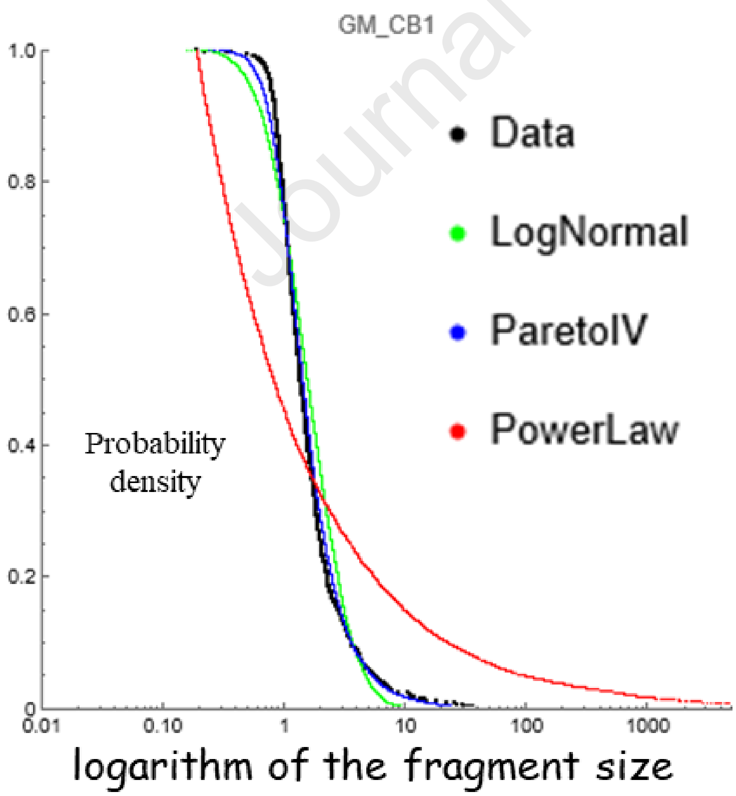

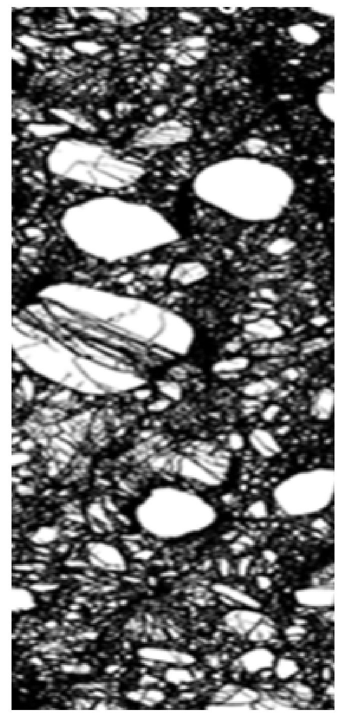

Linear and/or collisional fragmentation models provide similar results.

Fragment size distributions in brittle deformed rocks.

Alison Ord, Thomas Blenkinsop and Bruce Hobbs.

December_12_2021.

Abstract.

The production of breccias and cataclasites is commonly proposed to result in power-law or log-normal probability distributions for fragment (grain) size. We show that in both natural and experimental examples, the common best fit probability distributions for the complete distributions are members of the Generalised Gamma (GG), Extreme Value (GEV) and Pareto (GP) families; power-law and log-normal distributions are commonly, but not always, poor fits to the data. An hierarchical sequence, GG → GEV → GP, emerges as the sample mean of the fragment size decreases. The physical foundations (self-similar fragmentation, collisional fragmentation, shattering) for these distributions are discussed. Particularly important is the shattering continuous phase transition that results in the simultaneous development of both coarse fragments and ultra-fine particles (dust). This phase transition leads to Generalised Pareto fragment size distributions for the coarse fragments. Also included is a discussion of the relations between fragment size distribution, processes and deformation history in the context of monomineralic rocks. The overall reported size distributions are compatible with theoretical developments but the topic would benefit from observations and experiments conducted with the theories in mind.

Keywords

Fragment size distributions; breccias, cataclasites; Power-law, log-normal distributions; Generalised Gamma, Extreme Value, Pareto family distributions; linear and/or collisional fragmentation models.

1. Introduction.

Fragmentation is the breakage of a coherent structure into many pieces. In turn, each piece undergoes further fragmentation as the deformation continues; the mechanism of breakage may or may not involve collisions with other particles. The interest in fragmentation in the geosciences lies in understanding the mechanisms for formation of breccias, cataclastic shear zones, ejecta from impact sites and grain sizes in rocks in general. We are interested in this paper in the first two which are dynamic phenomena in the sense that the size distribution evolves with time (strain). The formation of breccias and cataclasites also involves processes other than breakage such as chemical reaction and dissolution at fragment contacts, further grinding, milling or wear, fragment rotation and perhaps removal of finer size fractions by dissolution, transport by shearing and melting. From a thermodynamic point of view, dissipation results from fragmentation, wear, chemical reaction/dissolution and frictional sliding whereas energy is absorbed by increases in surface area (finer grain-size). Thus we expect that the competition between dissipation and absorption of energy may become important as the grain size decreases.

The situation is made more complicated in that, especially at high temperatures and slow loading rates, the processes involved may not be entirely brittle but involve viscous effects. Thus the geological fragmentation process is multi-scaled with multiple, scale-dependent mechanisms operating. We are interested in the answers to the following questions: (1) *What is (are) the mechanism(s) for fragmentation in deforming rocks?* (2) *How are these mechanisms expressed in the observed probability distributions for fragment size?* (3) *Can we use such probability distributions to distinguish between pure shearing, simple shearing or more general deformation histories*?

There has been considerable discussion in the geological literature as to the forms of the fragment-size probability distribution that exists in these rocks. Some (Turcotte, 1986 a, b; Sammis et al., 1987; Ashby and Sammis, 1990) argue for a fractal (power-law) distribution; others (Phillips and Williams, 2021) argue for a log-normal distribution. In the physics literature other distributions are favoured including the Mott distribution and the Weibull (the Rosin-Rammler) distribution. In fact the Weibull distribution is one of the earliest empirical probability distributions put forward to represent fragment sizes; the Mott equation is a special form of the Weibull distribution. Phillips and Williams (2021) explored the stretched exponential distribution, which is the complementary cumulative Weibull distribution, but favoured the log-normal distribution. In Section 2 of this paper we show that the geometrical way in which an otherwise continuous body is divided into smaller pieces exerts a sensitive control on the resulting size probability function. Some fragmentation methods reproduce observed distributions and others do not. In this paper, instead of attempting to fit data to a preferred probability distribution we ask the question: *From a library of probability distributions, which one fits the observed data best?* The answer turns out to be *Generalised Gamma, Generalised Extreme Value* and *Generalised Pareto* distributions with power-law and log-normal distributions as relatively poor fits. However we emphasise that the approach is not simply a "best-fit curve fitting exercise". We require ideally that the best-fit distribution should also be compatible with theoretical models of the breakage process.

In Section 2 we review previous work on fragmentation; and place this work in the context of the relation between deformation processes and probability distributions in Section 3. Section 4 examines probability distributions for a number of published studies. The paper continues with a discussion of results in Section 5 and conclusions are drawn in Section 6.

2. Previous work.

Many models of fragmentation have been proposed in the literature. For detailed discussions see Grady (2006), Levy (2010) and Dadoun (2019). The discussion below is meant to emphasise that the precise mode of fragmentation exerts a sensitive control on the resulting probability distribution for particle size.

One of the first modern studies of fragmentation was by Rosin and Rammler (1933) who proposed, empirically, a probability distribution that was soon after described by Weibull (1939) and is now known as the Rosin-Rammler or Weibull distribution. The cumulative fraction greater than size, s, proposed by Rosin and Rammler (1933) is

$$F(s) = 1 - \exp\left[-\left(\frac{s}{s_0}\right)^{\beta}\right] \quad (1)$$

Here, s is the cumulative size of all particles of size greater than s, s_0 is a characteristic size, and the exponent β is a shape parameter. (1) has been used extensively, but pragmatically, since 1933. There are many attempts to base (1) on geometrical and physical principles, one of which is Lienau (1936) who developed a one-dimensional model consisting of a line divided randomly into segments of variable length, l (Figure 1a). He developed the cumulative distribution for an infinite line:

$$F(l) = 1 - \exp\left(-\frac{l}{l_0}\right) \tag{2}$$

If the line is finite of length, L, with the number of fragments, N_f, then the cumulative distribution is:

$$F(l) = 1 - \left(1 - \frac{l}{L}\right)^{N_f - 1} \tag{3}$$

Kolmogorov (1941) showed that if a structure is progressively fragmented such that each new fragment size, d, is independent of the immediately preceding fragment size (that is, the process is random), then a log-normal distribution results:

$$F(s) = s^{-1} \exp\left(-\chi (\log s)^2\right) \tag{4}$$

where χ is a constant.

Schuhmann (1941) pointed out that for small fragments, (4) reduces to

$$F(s) \sim \left(\frac{s}{s_0}\right)^{\beta} \tag{5}$$

which is a power law distribution interpreted by many to reflect a scale free or fractal geometry. Such a relation has been used by many authors including in particular Turcotte (1986 a, b) and Sammis et al. (1987). The relation between expressions (4) and (5) is important: if one truncates a distribution so that it approximates a power-law, then increasing the upper threshold, so that the contribution from coarser grains increases, can result in a log-normal distribution.

Mott and Linfoot (1943) developed 2D models (Figure 1 b, c) based on the Lienau, (2), distribution. In one of the simplest of these (Figure 1b), the spacing between fractures in the x- and y-directions follows Lienau distributions with different values for the parameter, N_f. More complicated models were developed (Grady, 2006), one of which, shown in Figure 1(c), consists of fractures in both the x- and y- directions with different Lienau distributions for both spacing and orientation.

Mott and Linfoot (1943) proposed a cumulative fragment distribution for the fragment mass, m, of the form

$$F(m) = 1 - \exp\left[-\left(\frac{m}{m_0}\right)^{1/2}\right] \tag{6}$$

which is again in the form of a Weibull distribution.

These geometrical approaches to fragmentation were extended by Grady and Kipp (1985) with the conclusion that although Weibull-type statistics may be common, the ultimate fragment size distribution depends on the rules that are proposed to describe the fragmentation process.

As indicated above, Kolmogorov (1941) examined the situation where the particle size at any instant is independent of the previous particle size in the instant before and showed that the resulting grain size distribution is log-normal. He pointed out that if the particle size were to be a power-law function of the previous particle size then other distributions would result. The point is that the grain size distribution that ensues during the breakage process is a direct result of the way in which the fragment size is related to the immediately previous fragment size. Clearly, many such ways are possible. The law that describes the way in which grain sizes are related from one increment of breakage to the next is called a *fragmentation kernel* (Pitman, 1999). The Kolmogorov result was generalised by Filippov (1961) who examined fragmentation processes where the fragmentation kernel is a power-law function of the fragment size and showed that a *generalised gamma* distribution results. The probability density function has the form:

$$F(x) = \frac{\beta}{\Gamma(k)\theta}\left(\frac{t}{\theta}\right)^{k\lambda-1} \exp\left[-\left(\frac{t}{\theta}\right)^{\lambda}\right] \qquad (7)$$

where $\theta > 0$ is a scale factor, and $\lambda > 0$, $k > 0$ are shape parameters. $\Gamma(k)$ is the gamma function, $\Gamma(k) = (k-1)!$, for any positive integer, *k*. The addition of erosion (by wear) does not change this distribution (Dadoun, 2019). In other words, according to this approach, processes that continuously decrease the fragment size in a power-law manner seem to preserve a generalised gamma distribution.

The generalised gamma distribution, (7), takes many forms. If we write $\omega = \frac{1}{\sqrt{k}}$ and $\sigma = \frac{1}{\beta}$, then ω = 0 gives a log-normal distribution, ω = 1 gives a Weibull distribution, $\omega = \sigma$ = 1 gives an exponential distribution, $\omega = \sigma$ gives a gamma distribution, and ω = -1 gives a Fréchet distribution. The generalised gamma distribution is also known as the Amoroso distribution (Crooks, 2010) which includes at least 50 distributions as special cases.

Bertoin (2001, 2002, 2006) and Bertoin and Gnedin (2004) embellish the Filippov model by proposing that the fragmentation process is characterised in terms of (i) an erosion coefficient that accounts for the reduction of particle size by processes (wear and dissolution of individual fragments) other than breakage, (ii) a dislocation rate that describes the rate (taken to be self-similar) at which fragmentation occurs and (iii) an index of self-similarity which describes the self-similar nature of the fragmentation process (Figure 1e). Again a generalised gamma distribution ensues and these three parameters characterise the details and type of the resulting distribution. Other mechanisms that continue to reduce the particle size other than fragmentation are chemical reactions and pseudotachylite formation (Magloughlin, 1992). Blenkinsop (1991) describes the corrosion of feldspars at fragment boundaries by the production of laumontite. Kaneko et al. (2017) describe chemical reactions in cataclasites and mass removal by fluid transport. Montheil et al. (2020) give examples of melting of fine grains in a pseudotachylite. It is useful to make the distinction between the processes of *wear* and *breakage*. Wear means removal of parts of the surface of a fragment by erosion, dissolution and chemical reactions; breakage means the separation of a fragment into two or more new fragments. The literature on fragmentation is well developed; that on wear (Bertoin (2001, 2002, 2006), Bertoin and Gnedin (2004)) needs considerable development.

Other models of fragmentation, which are special forms of the geometrical approach of Mott, include Turcotte (1986 a, b) and Sammis et al. (1987) who propose that each new fragment size is some proportion of the previous grain size with and without retention of some of the previous grain sizes. This means that the grain size decreases in an exponential manner with time and the result is a power-law (interpreted as a fractal) distribution of grain sizes. Other similar models are by Steacy and Sammis (1991) and Palmer and Sanderson (1991). A different model is by Brown and Wohletz (1995) who propose a self-similar model of breakage (Figure 1e) and arrive at a Weibull distribution; this approach is a sub-set of the Filippov approach.

However, other factors have been documented in cataclasites that preserve the grain size or decrease the probability that fracturing continues. Two of these processes (Einav, 2007a, b) are (i) cushioning of large particles by smaller particles so that the larger particles do not fragment further but smaller ones do and (ii) larger grains store more elastic energy than smaller particles so that once a small grain size forms it is less likely to fracture.

A particularly successful approach has been to follow Filippov (1941) and extend his kinetic approach. Recent approaches to fragmentation can be understood in terms of various versions of Filippov's fragmentation equation. The simplest version of this can be expressed as

$$\boxed{\begin{array}{l}\text{Rate of change of}\\ \text{concentration of}\\ \text{particles of size } k\end{array}} = -\boxed{\begin{array}{c}\text{Rate at which } k\text{-sizes are broken into}\\ \text{smaller sizes}\end{array}} + \sum \boxed{\begin{array}{c}\text{Rates at which fragments larger than } k\\ \text{are broken into } k \text{ sizes}\end{array}} \qquad (8)$$

This version of the fragmentation equation (called a linear fragmentation model by Redner, 1989) can be elaborated to say that the rate at which the concentration, $c(x)$, of fragments of size, x, changes is equal to a depletion term:

$$-R(x)c(x)$$

and an augmentation term:

$$+\sum_{y}^{\infty} R(y)B(x\,|\,y)c(y)$$

where $R(x)$, $R(y)$ are the rates of fragmentation of fragments of sizes, x and y with $y > x$, and $B(x\,|\,y)$ is the average number of fragments of size x produced by fragmentation of larger fragments with sizes, y. $B(x\,|\,y)$ is normalised so that mass is conserved. The fragmentation equation (8) was solved by Filippov (1961) with the self-similar assumptions, $R(x) \propto x^{\lambda}$ $R(y) \propto y^{\lambda}$ and $B(x\,|\,y) \propto y^{\lambda}$, where λ is a power law exponent commonly called the *homogeneity index*. Filippov (1961) showed that the solution to (8) is a generalised gamma distribution. He also showed that if $\lambda < 1$ then the fragment size rapidly approaches zero leaving no large particles and only "dust". A geologist might interpret this as a form of pseudotachylite (with no melting).

Equation (8) applies to situations where the boundary conditions for the material are purely compressive so that the deformation history is a pure shearing. The fragmentation process can be expanded to include fragmentation by collision processes as may be the situation in simple shearing deformations. Now instead of (8) the collisional fragmentation process is written as (9) (Redner, 1989; Cheng and Redner, 1990). In order to solve this equation it is necessary to adopt simple, specific models of fragmentation, and solutions for three collisional models are given in Table 1. Note that gamma distributions are predicted for coarse grain sizes.

$$\boxed{\text{Rate of change of concentration of particles of size, } k} = -\boxed{\text{Rate of change due to collision of k-mers with any size particle}} + \sum \boxed{\text{Rate of gain of } k\text{-mers due to collision of particles with size greater than } k} \quad (9)$$

An important part of these analyses is the recognition of a continuous phase transition for $\lambda \leq 0$ (Krapivsky et al., 2017; Krapivsky and Ben-Naim, 2003). Here, the energy of the system is minimised by the simultaneous formation of two phases: coarse grains and a fine grained "dust" (Figure 2). Some of the various processes envisaged in theories of fragmentation developed to date are illustrated in Figures 2 and 3 and in Table 1.

In summary, a geometrical approach to fragmentation shows that the resultant fragment size distribution is sensitive to the geometrical fragmentation law proposed. If the process is random then a log-normal distribution results (Kolmogorov, 1941). If a geometrical series model is proposed a power-law distribution results (Turcotte, 1986, a, b; Sammis et al. 1987). Instead of a geometrical approach, a deeper insight into fragmentation is obtained from kinetic equations for the fragmentation process. If the kinetics are linear (controlled solely by boundary conditions, as may be the case for pure shearing deformations) then, for self-similar law breakage (where the breakage rate is proportional to the fragment size raised to an exponent, λ), a generalised gamma distribution results (Filippov, 1961). If $\lambda > 0$ (the largest fragments break faster than small ones) the distribution for larger fragments remains a generalised gamma whereas that for smaller fragments is log-normal if no wear occurs and power law if wear is present. If $\lambda < 0$ (smaller fragments break faster than large ones) then shattering occurs and the complete mass is rapidly converted to dust with no remaining large fragments.

For processes controlled solely by collision of particles (as may be the case for simple shearing) then the resulting grain size distribution depends on the details of the breakage model. For situations where $\lambda \geq 1$ and both large and small grains break, the large grains have a gamma distribution whereas the small grains are log-normal. If only the large grains fragment then the large grains have a gamma distribution and the small an exponential distribution. If only the small grains break then the large grains have a power-law distribution and the small a log-normal distribution. On the other hand, if $\lambda < 1$ (small grains break more readily than large), a continuous ("second order") phase transition occurs where the energy of the system is minimised by the simultaneous formation of large grains and small "dust". This is known as a shattering transition (Krapivsky and Ben-Naim, 2003; Krapivsky et al., 2017). Hence, the fragment size distribution that ultimately arises in a given situation is sensitive to the details of the breakage mechanisms and the history of such mechanisms. Deformation mechanisms may evolve over time, and cataclasites may preserve evidence of different stages. Any analysis of fragment size distributions in natural or experimental cataclasites needs to take this into account rather than simply postulate that the distribution is power-law, log-normal or some other preferred distribution.

It is also important to note that the type of distribution depends on the levels of truncation of the distribution or thresholding of the data. In practice there is always a lower cut-off, or *threshold*, in measuring the size distribution for fragments arising from the resolution of the measuring process. The question arises as to the influence of such a threshold? Clearly the threshold value changes the mean and variance of the sample and in particular changes the location and shape parameters where these quantities are relevant. In addition the value of the threshold can change the *type* of distribution. Thus for large thresholds, gamma and Gumbel distributions become light tailed exponential distributions and a Fréchet distribution becomes a heavy tailed Generalised Pareto distribution. A Weibull distribution can become a localised beta distribution. Thus the influence of the threshold depends on the type of un-thresholded distribution and on the level of the threshold. For some thresholds only the parameters of the distribution are affected, for others the type of distribution is affected. We note that the terms *truncation* of data and *thresholding* are used differently in the statistics literature. Truncation means that one retains the data but restricts the domain of the distribution. Thus the progressive restriction of the extent of a distribution so that the distribution changes from log-normal to power-law as described by Phillips and Williams (2021 Figure 2) is a process of *truncation*. The consideration of values only above a cut-off value as is the case if particle sizes below a certain value cannot be resolved is *thresholding*. The truncation process emphasises that different parts of a probability distribution can have their own distribution. There is a large literature on truncation and thresholding (Coles, 2001; Beirlant et al., 2005; Embrechts et al,. 1997; Gumbel, 1985).

3. Some comments on statistical distributions and processes operating during fragmentation.

We will see in Section 4 that more than one distribution can appear as a good fit to a given data set. An example is presented in advance in Figure 4 for data from Phillips and Williams (2021). The best fit here is Pareto Type II (Table 2) but Pareto Types I and IV are also close. Log-normal does not fit the data well. One can always quibble about which distribution is best and pragmatically (if one is not concerned with the physical processes that formed the distribution) one may prefer one distribution over another. However here we are interested in what an observed distribution or set of distributions might reveal about the underlying processes of fragmentation and so this section offers some comments about the processes that operate in breccia and cataclasite formation and the controls that a particular process can exert on the development of a particular probability distribution. We also comment on what is to be expected of a probability distribution as one moves further into the tail of a distribution.

The link between processes and probability distributions was made clear by Savageau (1979, 1980) who observed that: *Any system that grows into a stable mature form has a growth curve that is a legitimate cumulative probability distribution*. Savageau (1979, 1980) showed that, for interacting nonlinear systems, a general equation can be derived that describes the generation of a quantity of interest, X, combined with competition with other processes, to produce a generalised growth law for X. This equation includes many of the common growth laws (logarithmic, power-law, Weibull, stochastic, Gompertz and Lotka-Volterra) as special cases. His analysis emphasises that although a large number of processes may operate to produce the growth of a system, an overall simple pattern of growth may result. This concept is amplified by Frank (2009, 2011, 2014).

Rocha and Aleixo (2013) explore the interacting processes of growth and competition using a generalised growth model that describes the progressive evolution of a system where growth nucleates, and subsequent growth follows a symmetrical or asymmetrical sigmoidal curve to ultimate extinction. This is the Gompertz law:

$$f_{r,q,p}\left(x\right)=rx^{p-1}(1-x)^{q-1}$$

which is a generalisation of the simple logistic equation, widely used in population dynamics, for which $q = p = 2$. The Gompertz law describes the competition between an accelerating growing process and processes that tend to inhibit growth; it is attractive from a process point of view since it is used in various forms in material science (in the form of Kolmogorov–Avrami kinetics for recrystallisation; Martyushev and Axelrod, 2003) and as a form of kinetics for non-equilibrium chemical systems with coupling to both heat and fluid supply (Ord et al., 2012; Hobbs and Ord, 2018). As indicated above it is also one member of the more general growth laws discussed by Savageau (1979, 1980). Rocha and Aleixo (2013) show that the Generalised Extreme Value distributions: *Weibull*, *Gumbel* and *Fréchet*, are special cases of the Gompertz growth law.

The analyses by Savageau (1979, 1980) and Rocha and Aleixo (2013) involve systems where growth and one or more antagonistic processes operate. Other analyses involve only growth processes. Foremost here are Kolmogorov (1941) who showed that random fragmentation leads to a log-normal distribution, Filippov (1961) who showed that self-similar fragmentation leads to a Generalised Gamma distribution and Turcotte (1986 a, b)/Sammis et al. (1987) who showed that a geometrical series as a fragmentation law leads to a fractal (Pareto Type I) distribution.

Two principles govern the development of a specific probability distribution in physical, biological and chemical systems (Frank, 2011). First, a given distribution maximises entropy (or randomness) subject to the constraints imposed by the processes operating in the system. Frank (2014) shows that this constraint of maximum entropy means that all common probability distribution have the form

$$p_y \propto m_y \exp\left(-\varpi T_f\right)$$

where p_y is the probability density, m_y is a scale factor that expresses the way in which the probability distribution changes with measurement scale, ϖ is a constant related to the way in which entropy is maximised to produce p_y and T_f is a measurement scale (for instance, logarithmic or linear). See Frank (2014) for details.

The concept is that the multitude of random perturbations that affect the pattern development tend to cancel each other in the aggregate, leaving the system completely random except for any constraints that restrict the pattern. As an example, if the variance is constrained by the chemical/physical/genetic processes operating in the system then the distribution that maximises entropy is the Gaussian (Frank, 2009). Thus many environmental factors influence the growth of a human and perturb the growth rate but most cancel out and the growth is ultimately the result of genetic factors that severely restrict the variance of the height distribution. If the geometric mean is constrained then power-laws develop.

Second, different processes produce different relations between the magnitude of a quantity (grain-size, metal endowment) and the evolution of the magnitude with time. Two common evolutionary paths in natural systems are log-linear and linear-log paths. In log-linear paths, the system begins with logarithmic relations between magnitude and time and blends into a linear relation. The linear-log paths are the opposite (Figure 5). It is this kind of relation that defines each probability family within the various maximum entropy families. For example, since the gamma distribution, $p(y) = ky^{\alpha-1}\exp(-\varpi y)$, is the product of a power law, $y^{\alpha -1}$, and an exponential, exp(-ϖy); when the magnitude of y is small, the shape of the distribution is dominated by the power law component, y^{-c}. As the magnitude of y increases, the shape of the distribution is dominated by the exponential component, $e^{-\varpi y}$. Thus, the underlying measurement scale grades from logarithmic at small magnitudes to linear at large magnitudes. Indeed, the gamma distribution is the archetype expression of an underlying measurement scale that grades from logarithmic to linear as magnitude increases (Frank, 2014, Section 5). Variations in the transition between the logarithmic and linear regime describe nearly all of the variation in observed patterns (Frank, 2014).

Thus the log-linear relation defines the gamma, logarithmic and power law families; the linear-log relation defines the Gaussian and exponential distributions in the small-scale linear domain, and adds power law tails in the large scale logarithmic domain (Frank, 2011; 2014). Logarithmic scaling is an expression of multiplicative processes whereas linear scaling is an expression of additive processes (Frank, 2014). It should be noted that the gamma pattern differs most strongly from the lognormal by allowing a higher probability weighting of small values; otherwise, the lognormal and gamma distributions are similar.

Many processes may be essentially multiplicative at small scales and approximately linear at large scales. All such generative processes will also converge to the gamma probability distribution. In the general case, k is a continuous parameter that influences the magnitudes at which logarithmic or linear scaling dominates. k is obtained from $p_y \propto y^{k-1}\exp(-\alpha y)$. Thus it is not surprising that the generalised gamma distribution can be approximated by some 50 different distributions (Crooks, 2010); each approximation corresponds to a different value of k marking the transition from logarithmic to linear scaling. It is noteble that the Gompertz distribution is not part of the generalised gamma family and we return to this in the discussion. The common probability distributions identified in natural and experimental fragmentation systems are summarised in Table 2.

Throughout the following section, we use the following groups of terms interchangeably: (power-law, Pareto, Pareto Type I, Pareto2), (Pareto Type II and Pareto3), (Pareto Type IV and Pareto4). See https://reference.wolfram.com/language/ref/ParetoDistribution.html for usage. Terms such as Fréchet2(3) mean the two (three) parameter Fréchet distribution.

4. Observations on natural and experimentally deformed samples.

In this section we present best fit probability distributions for eight published studies of fragment sizes in naturally and experimentally deformed breccias, cataclasites and a pseudotachylite. Only brief results are given; the closest fits are given in the Appendix and an array of distributions is given in the Supplementary Material. In all, at least 800 fragment size probability distributions were calculated. The data for Phillips et al. (2020), Melosh et al. (2014), Hadizadeh et al. (2010), Fagereng (2011), and Marone and Scholz (1979) were all obtained from Phillips and Williams (2021; their repository *10 .17605 /OSF.IO /JDW8N*). The data are analysed using Mathematica 12.3.1 (Wolfram Research 2021).

4.1. Phillips et al. (2020).

Phillips et al. (2020) studied altered shale and basalt samples which were experimentally sheared at 150°C. For the analyses conducted in this paper all samples (Phillips and Williams, 2021) are fitted very closely by a Pareto Type II distribution (Figure 6; see also Supplementary Material). Figure 6 (a, b) shows that Pareto Type IV is also sometimes a close fit whereas log-normal shows strong departures from the data especially at medium to small grain sizes. Figures 6 (c, d) show the Pareto Type II fit to the N_ABB data alone for clarity. An example is presented in Figure 6 (e, f) for the data set N_ABB where Mathematica indicates the distribution of best fit is given by the Pareto Type II distribution: Figure 6(e) shows the raw data on a linear-linear plot whereas Figure 6(f) shows the distribution on a log-log plot. Note that the log-log plot for the raw data is concave downwards similar to that interpreted as “bi-fractal” by many authors in natural data sets. We suggest that many “fractal” or “bi-fractal” distributions in the literature may in fact be Pareto Type II distributions.

4.2. Melosh et al. (2014).

Melosh et al. (2014) explored a natural breccia system in which there has been little relative movement of fragments so that there has been little wear. There is a transition from intact rock to a crackle breccia to a mosaic breccia and finally what the authors call a chaotic breccia. This represents a transition from unbroken rock to the early stages of breccia formation. This progressive development of breccia is represented by a transition from slightly scattered fragment size distributions for the crackle breccias (PSKB through to PS194b in Figure 7) to tightly defined distributions in the mosaic/chaotic breccias (PS197 to PS126 in Figure 7). In all cases however the fragment size distributions are well fitted by members of the Generalised Pareto or Generalised Extreme Value families. The Generalised Gamma is also a good fit for some. The Pareto Type I (power-law) and log-normal distributions are not good fits.

4.3. Hadizadeh et al. (2010).

The Hadizadeh et al. (2010) data sets come from small displacement natural faults (minimum shear strain ≈14) and from shear displacement experiments (minimum shear strain ≈22), both comprised of sandstone specimens. The data for the natural examples are well fitted by any of Gamma4, Pareto4 and Fréchet3. Log-normal is a good fit also for one distribution. An example is shown in Figure 8.

4.4. Fagereng (2011).

The Fagereng (2011) data sets are from a mélange zone in the Otago Schists and consist of fragment size distributions from both outcrop and thin section scales. The Fréchet2 and 3 distributions are the best fits.

4.5. Blenkinsop (1991).

The Blenkinsop (1991) data sets come from the Cajon Pass drill hole through the San Andreas Fault in California. Fragments have developed without rotation or shear. Deformation is coupled with chemical reactions whereby plagioclase is replaced by laumontite. The fragment size distributions differ from others examined here in that the Gompertz distribution is strongly represented (Figure 10) along with the Generalised Gamma and Gumbel2.

4.6. Marone and Scholz (1979).

The Marone and Scholz (1979) data sets are from experimentally sheared quartz sands with shear strains between 0 and 3.3%. Some of the microstructures developed are shown in Figures 2 and 3. Some fragment size distributions are shown in Figures 11 where Fréchet2 followed by Generalised Gamma are best fits.

4.7. Ferreira and Coop (2020).

The Ferreira and Coop (2020) data sets come from ring shear experiments on initial sands (see also Coop et al.,2004). Shear strains from 440% to 44500% are reported so that these are by far the highest experimental strains explored here. At lowest strains (Figure 12 a, b) a Fréchet2 distribution is the best fit. At intermediate strains (6940%; Figure 12 c, d) this is replaced by Pareto Type I whilst at the highest strain (Figure 12 d, e) the best fit is Gamma4. It is interesting that Gamma4 is also a reasonable fit for the lower strains especially for the largest grain size fraction.

4.8. Montheil et al., 2020.

The Montheil et al. (2020) data sets come from experimentally produced pseudotachylites, the initial rocks being tonalite and granite. Both glass and fine grained fragments are produced and the latter are analysed here. There is evidence of melting at fragment boundaries. The best fit distributions for these data sets are Fréchet2, Fréchet4 and Pareto Type IV. We show these in Figure 13 together with some others that are poor fits

5. Discussion.

The data examined in this paper span samples that range from low strain mosaic breccias through to fine fragments in pseudotachylite and to very high strain breccias. Although a unique distribution in general cannot be established for many data sets most are expressed as Generalised Gamma distributions or members of the Generalised Extreme Value or Generalised Pareto families.

The theoretical discussions of fragmentation considered in Section 2 propose that Generalised Gamma distributions should be common especially for the coarse grained fractions of probability distributions. However others are to be expected and the challenge is to see how closely observed fragment size distributions in deformed rocks fit the theory. The issue is that the theoretical analyses are idealised in the sense that only simplified models of fragmentation are considered and some processes such as chemical reactions and melting are not considered. It is also noteworthy that no theoretical studies deal with polymineralic materials. The hope is that observations on deformed rocks will either confirm these models or suggest modifications that can be incorporated into the theory.

A first observation is that the power-law (Pareto Type I) or the log-normal distributions hardly appear in the distributions for any data set even though they are extremely popular in the geological literature. This is partly because many fits to data sets in the literature truncate the distributions by selecting only the central part of the distributions for analysis and discard the tails of the distributions. This is somewhat unfortunate because most of the information on the processes of fragmentation lie in the tails in that the distributions (Nair et al., 2021) can have exponential (for a power-law distribution), sub-exponential (for a log-normal distribution) or regularly varying decay (for a Gamma or Extreme Value distributions) in the tails depending on the mechanism of fragmentation. The remainder of the distribution, after discarding the tails, is an approximately linear distribution on a log-log plot which is assumed to be a physically meaningful power-law. If the selected part of the distribution is extended into the coarser fraction it can be close to a log-normal distribution. When the complete distributions (that is, inclusion of the tails) are taken, Pareto Type I and log-normal distributions are rare.

As indicated, it is commonly difficult to select a unique best fit distribution for a given data set. This arises because a given set of parameters for a given probability distribution can produce a distribution which is identical or very similar to that of a different family. Thus for the Blenkinsop (1991) data set 6241.3NX20X (Figure 14), a Generalised Gamma distribution with parameters [a = 0.246529, p = 4.82455, d = 32.3683] and a position parameter of -2.34208 is almost identical to a Gompertz distribution with parameters [η = 2.76893, b = 0.00509909] even though the Gompertz distribution is not part of the Generalised Gamma family (Crooks, 2010). For this reason we want to distinguish between those distributions that arise from known mechanisms of fragmentation (those discussed in Section 2) and those that arise by chance and have no known mechanism associated with them. The first of these we call *fundamental distributions* and the second, *incidental distributions*.

The tables of results given in the Appendix and the results in Supplementary Material show that the Generalised Gamma distribution is the best fit for most of the data sets examined. However as the grain size decreases other distributions (in particular, Generalised Extreme Value distributions such as Fréchet and generalised Pareto such as Pareto Type IV) appear. There seems to be an overall hierarchy proceeding from Generalised Gamma at coarse grains to Fréchet as the grain size decreases to Generalised Pareto distributions in pseudotachylites. This is broadly in agreement with Table 1 but the progression is not as clear cut as in Table 1.

As to the questions raised in the Introduction:

(1) *What is (are) the mechanism(s) for fragmentation in deforming rocks?* The literature so far has examined three different models of fragmentation: Random breakage (Kolmogorov, 1941) leading to log-normal distributions, linear breakage (Turcotte, 1986 a, b; Sammis and King, 1997) leading to power-law distributions and non-linear breakage characterised by self-similar fragmentation laws (Filippov, 1961; Cheng and Redner, 1990) leading to Generalised Gamma distributions for coarse fragments and a range of other distributions (Table 1) depending on fragment size and details of the breakage model. The observation that many fragment distributions are Generalised Gamma distributions is compatible with self-similar fragmentation as indicated in Section 2 and Table 1. Such a distribution is to be expected for coarse particles from both continuous fragmentation and fragmentation involving collision. The dominance of Extreme Value Distributions (Fréchet in particular) for fine particles is not directly compatible with Table 1. However, Fréchet distributions (and other Extreme Value Distributions) distributions, together with power-law and log-normal are members of the Generalised Gamma distribution (Crooks, 2010) so that it is reasonable to infer that self-similar fragmentation is dominant down to the finest fragment sizes measured to date. The observation that the probability of fracturing decreases as the fragment size decreases (Figure 14) is also compatible with a non-linear breakage model and with the observation of Einav (2007 a, b) that the driving force for breakage (elastic energy) decreases with decrease in fragment size. A non-linear breakage mechanism also predicts a shattering phase transition which seems to be common perhaps in shearing deformations (Figures 2 and 3). The processes that have not yet been incorporated into fragmentation models are cushioning of coarse fragments by fine particles (Figure 3 and Einav, 2007, a. b) and the effect of chemical corrosion and melting.

Although the Generalised Gamma distribution is a reasonable fit for some data sets the correspondence to a self-similar fragmentation model as assumed by the theory is a little problematic. The best fits are for the Blenkinsop data where values of the homogeneity index, λ, are derived to be in the range 3 to 7 with an average of about 4 (Table 3). This seems to be a little high since it implies that a two-fold decrease in fragment size results in a 16-fold decrease in fracture number per grain. Figure 15 would suggest a value for λ less than 4 (perhaps closer to 2). On the other hand the value of λ for the Montheil et al. data for fragmentation of granite is zero, compatible with a shattering transition. Clearly more carefully designed experiments are needed to confirm if the theory is applicable.

(2) *How are these mechanisms expressed in the observed probability distributions for fragment size?* As indicated above, the random Kolmogorov breakage model appears not to be relevant since log-normal distributions are rare except for truncated data. Similarly the linear Turcotte-Sammis models predict power-law (Pareto Type I) distributions which are rarely observed except again for truncated data. Non-linear (Filippov-Cheng-Redner) breakage models based on self-similar breakage kernels are consistent with the Generalised Gamma distributions observed. There appears to be a hierarchy of distributions ranging from Generalised Gamma to Generalised Extreme Value to Generalised Pareto as the sample mean decreases. It may be that this hierarchy is

expressed as a progressive change in the parameters that describe the Generalised Gamma but we have not explored this. The existing models do not account for the possibility that the homogeneity index, λ, changes with increasing strain so that the number of fragments produced from a single grain changes as the strain increases but no model so far takes this into account. There is also the possibility that a simple power law is not sufficient to explain the fragmentation process and other nonlinear fragmentation kernels are relevant.

(3) *Can we use such probability distributions to distinguish between pure shearing, simple shearing or more general deformation histories*? There is no strong evidence in the results of this paper that the deformation history produces differences in the fragment probability distribution. The low strain crackle breccias of Melosh et al. (2014; Figure 7 of this paper) indicate gamma distributions for most specimens with Pareto 4 and Fréchet dominating in the most chaotic of breccias whereas the very high shear strain specimens of Ferreira and Coop (2020; Figure 11 of this paper) are best fit by a gamma distribution. Perhaps future carefully designed experiments will reveal history dependent distributions, especially in the details of the parameters that define the distributions.

6. Conclusions.

An assumption in much of the geological literature is that fragment size distributions should be power law (Pareto Type I) or log-normal distributions. To this end observed fragment size distributions are truncated so that the tails are neglected and only the central part of the distribution is analysed. This results in power law or log-normal distributions depending on how much of the coarse fraction is included. This is the difference between the Kolmogorov (1941) and Schuhmann (1941) results (see expressions (4) and (5)). In fact power-law or log-normal distributions are poor fits to observed distributions if all the data are taken into account. All measured distributions from natural and experimental specimens are downward concave or sigmoidal shaped in log-log plots and if the complete distribution is considered the result is invariably a Generalised Gamma distribution if the fragment size is coarse or Fréchet/Pareto IV distributions if the fragment size is small (as in pseudotachylites). These results are broadly compatible with the results of theory (Table 1) for self-similar fragmentation with either or both linear or collisional fragmentation models. In general it is difficult to define a unique probability distribution for a given data set and other distributions are just as likely from analysis including members of the Generalised Extreme Value, Generalised Pareto and Gompertz families. However only the Generalised Gamma family is consistent with theory and we propose that the other distributions appear only incidentally. There is much work still necessary to relate fragment probability distributions to process including whether a continuous phase transition in the form of a shattering transition exists. Such a transition would explain the initiation of those pseudotachylites comprised largely of fragments. Melting may yet turn out to be another phase transition. Deformation mechanisms may evolve over time, and cataclasites may preserve evidence of different stages. Fundamental distributions still need to be developed to take into account polymineralic materials. Investigating fragmentation mechanisms in most geological materials will be hampered until this is achieved.

Acknowledgments.

We thank Matthew Coop, Leny Montheil and Virginia Toy for access to data. Eunhyun Park from Wolfram Technical Support is thanked for help in understanding the Mathematica code for probability distributions. We are grateful to Peter Eichhubl and two other anonymous reviewers for their useful comments.

Data

The data for Fagereng (2011), Hadizadeh et al. (2010), Marone and Scholz (1989), Melosh et al. (2014) and Phillips et al. (2020) were downloaded from the repository described by Phillips & Williams (2021), Acknowledgments, Samples, and Data, of 10 .17605 /OSF.IO /JDW8N

References.

Arnold, B. C. 1983. Pareto Distributions. International Cooperative Publishing House, Fairland, Maryland USA.

Ashby, M.F., Sammis, C.G. 1990. The damage mechanics of brittle solids in compression. Pure and applied geophysics 133, 489-521.

Austin, L. G., Luckie, E. T., Klimpel, R. R. 1972. Solutions of the batch grinding equation leading to Rosin-Rammler distributions. Trans. Soc. Min. Engr. AIME. 252, 87-94.

Bajzer, Z. 1999. Gompertzian growth as a self-similar and allometric process. Growth, Development and Aging. 63, 3 – 11.

Blenkinsop, T.G., 1991. Cataclasis and processes of particle size reduction. Pure Appl. Geophys. 136, 59–86.

Beirlant, J., Goegebeur, Y., Segers, J., Teugels, J. 2005. Statistics of Extremes. Theory and Applications. John Wiley & Sons Ltd. 490p

Bertoin, J, 2006. Random Fragmentation and Coagulation Processes. Cambridge.

Bertoin, J. 2002. Self-similar fragmentation. Ann. I. H. Poincaré. 38, 319 – 340.

Bertoin, J. 2001. Homogeneous fragmentation processes. Probab. Theory Relat. Fields. 121, 301-318.

Bertoin, J., Gnedin, A, V. 2004, Asymptotic laws for nonconservative self-similar fragmentations. Electronic Journal of Probability. 9, 575 – 593.

Brown, W. K, Wohletz, K. H. 1995. Derivation of the Weibull distribution based on physical principles and its connection to the Rosin–Rammler and lognormal distributions. J. Appl. Phys. 78, 2758–2763.

Cheng, Z., Redner, S, 1990. Kinetics of fragmentation. J. Phys. A 23, 1233.

Coles, S, 2001. An Introduction to Statistical Modeling of Extreme Values. Springer Series in Statistics. Springer Verlag London. 208p

Coop, M. R., Sorensen, K. K., Freitas, B., Georgoutsos, G. 2004. Particle breakage during shearing of a carbonate sand. Geotechnique 54, 157–163.

Crooks, G. E. 2010. The Amoroso Distribution. Technical Notes, Physical Biosciences Division, Lawrence Berkeley National Lab, Berkeley.

Dadoun, B, 2019. Some Aspects of Growth-Fragmentation. Thesis. University of Zurich. Some Aspects of Growth-Fragmentation - TEL - Thèses en ligne (archives-ouvertes.fr)

Einav, I. 2007a. Breakage mechanics - part I: theory. J. Mech. Physics Solids 55, 1274-1297.

Einav, I. 2007b. Breakage mechanics - part II: modelling granular materials. J. Mech. Physics Solids. 55, 1298-1320.

Embrechts, P., Klüppelberg, C., Mikosch, T. 1997. Modelling Extremal Events for Insurance and Finance. Springer Verlag Heidelberg.

Fagereng, Å., 2011. Frequency-size distribution of competent lenses in a block-in-matrix mélange: imposed length scales of brittle deformation? J. Geophys. Res. 116.

Ferreira, P. M. V., Coop, M. R. 2020. Factors that influence the terminal grading of sands. Géotechnique Letters 10, 518–523.

Filippov, A. F. 1961. On the distribution of the sizes of particles which undergo splitting. Theory of Probability and its Applications, 6, 275 – 294.

Frank, S. A. 2014. How to read probability distributions as statements about process. Entropy 16, 6059-6098.

Frank, S. A. 2011. Measurement scale in maximum entropy models of species abundance. Jour Evolutionary Biol. 24, 485 – 496.

Frank, S. A. 2009. The common patterns of Nature. Jour. Evolutionary Biology. 22, 1563–1585.

Grady, D, E. 2006. Fragmentation of Rings and Shells: The Legacy of N.F. Mott. Springer.

Grady D.E., Kipp, M. E, 1985. Geometric statistics and dynamic fragmentation. Journal of Applied Physics 58, 1210-1222.

Gumbel, E. J. 1958. Statistics of Extremes. (Dover Publication, New York 2004).

Hadizadeh, J., Sehhati, R., Tullis, T. 2010. Porosity and particle shape changes leading to shear localization in small-displacement faults. J. Struct. Geol. 32 (11), 1712–1720.

Harris, T. 1963. The Theory of Branching Processes. Springer.

Hobbs, B.E., Ord, A. 2018. Episodic modes of operation in hydrothermal gold systems: Part II. A model for gold deposition. In:: Gessner, K., Blenkinsop, T. G., Sorjonen-Ward, P. (eds) Characterization of Ore-Forming Systems from Geological, Geochemical and Geophysical Studies. Geological Society, London, Special Publications, 453, https://doi.org/10.1144/SP453.15

Kaneko, Y., Takeshita, T., Watanabe, Y., Norio Shigematsu, N., Fujimoto, K-I. 2017. Alteration Reaction and Mass Transfer via Fluids with Progress of Fracturing along the Median Tectonic Line, Mie Prefecture, Southwest Japan, Chapter 6 117 – 138. In: Evolutionary Models of Convergent Margins- Origin of Their Diversity. IntechOpen.

Kolmogorov, A. N. 1941. Über das logarithmisch normale Verteilungsgesetz der Dimensionen der Teilchen bei Zerstückelung. *Dokl. Akad. Nauk. SSSR* 31, 99–101. Translated as: On the logarithmic normal distribution of particle sizes under grinding. Paper 29, In: Selected Works of A. N. Kolmogorov, Volume II. 1992. Editor: A. N. Shiryayev. Springer.

Krapivsky, P. L., Otieno, W., Brilliantov, N, V. 2017. Phase transitions in systems with aggregation and shattering. Phys. Rev. E, 96, 042138.

Krapivsky, P. L., Ben-Naim, E. 2003. Shattering transitions in collision-induced fragmentation. Phys Rev E Stat Nonlin. Soft Matter Phys, 68, 021102.

Levy, S. 2010. Exploring the Physics behind Dynamic Fragmentation through Parallel Simulations. PhD Thesis No.4898. École Polytechnique Fédérale de Lausanne. https://www.researchgate.net/publication/47355624_Exploring_the_Physics_behind Dynamic_Fragmentation_through_Parallel_Simulations.

Lienau, C.C. 1936. Random fracture of a brittle solid. Journal of the Franklin Institute 221, 485-494; 673-686; 769-787.

Magloughlin, J. F. 1992. Microstructural and chemical changes associated with cataclasis and frictional melting at shallow crustal levels: the cataclasite-pseudotachylite connection. Tectonophysics, 204, 243-260.

Marone, C., Scholz, C.H. 1979. Particle-size distribution and microstructures within simulated fault gouge. J. Struct. Geol. 11, 799–814.

Martyushev, L.M., Axelrod, E.G. 2003. From dendrites and S-shaped growth curves to the maximum entropy production principle. JETP Letters, Vol. 78, No. 8, 2003, pp. 476–479. From Pis'ma v Zhurnal Éksperimental'noœ i Teoreticheskoœ Fiziki, Vol. 78, No. 8, 2003, pp. 948–951.

McGrady, E. D., Ziff, R. M. 1987. Shattering transition in fragmentation. Phys. Rev. Lett. 58, 892 - 895.

Melosh, B.L., Rowe, C.D., Smit, L., Groenewald, C., Lambert, C.W., Macey, P., 2014. Snap, crackle, pop: Dilational fault breccias record seismic slip below the brittle – plastic transition. Earth Planet. Sci. Lett. 403, 432–445.

Montheil L, Toy V. G, Scott J. M, Mitchell T. M., Dobson D. P. 2020. Impact of coseismic frictional melting on particle size, shape distribution and chemistry of experimentally generated pseudotachylite. Front. Earth Sci. 8:596116.

Mott, N. F., Linfoot, E. H. 1943. A theory of fragmentation. United Kingdom Ministry of Supply AC3348.

Nair, J., Wierman, A., Zwart, B. 2021. The Fundamentals of Heavy Tails: Properties, Emergence, and Estimation. Unpublished. Available at: https://adamwierman.com/book/.

Nguyen, G. D., Einav, I. 2009. The energetics of cataclasis based on breakage mechanics. Pure Appl. Geophysics 166, No. 10, 1693-1724.

Ord, A., Hobbs, B.E., Lester, D.R. 2012. The mechanics of hydrothermal systems: I. Ore systems as chemical reactors. Ore Geology Reviews 49, 1-44.

Palmer, A.C., Sanderson, T.J.O. 1991. Fractal crushing of ice and brittle solids. Proc. R. Soc. Lond. A 433, 469-477

Phillips, N. J., Belzer, B., French, M. E., Rowe, C. D., Ujiie, K. 2020. Frictional strengths of subduction thrust rocks in the region of shallow slow earthquakes. Journal of Geophysical Research: Solid Earth, 125

Phillips, N. J., Williams, T. T. 2021. To D or not to D? Re-evaluating particle-size distributions in natural and experimental fault rocks. Earth and Planetary Science

Letters. 553, 116635.
Pickands, J. III. (1975). Statistical inference using extreme order statistics. Annals of Statistics, 3, 119-131.
Pitman, J. 1999. Coalescents with multiple collision. Ann. Probab. 27, 1870-1902.

Redner, S. 1989. Statistical theory of fragmentation. Chapter 6, pp 31 - 48 in: Disorder and Fracture. Eds J. C. Charmet, S. Roux and E. Guyon. Plenum Press, London.

Redner, S. 1990. Statistical Models for the Fracture of Disordered Media, Eds H. J. Herrmann and S. Roux. North-Holland.

Rocha, J. L., Aleixo, S. M. 2013. An extension of Gompertzian growth dynamics; Weibull and Fréchet models. Mathematical Biosciences and Engineering. 10, 379 – 398.

Rosin, P., Rammler, E. 1933. The laws governing the fineness of powdered coal. Journal of the Institute of Fuel 7, 29–36.
Sammis, C. G., King, G. C. P., Biegel, R. 1987, The kinematics of gouge deformation, Pure Appl. Geophys., 125, 777– 812.
Sammis, C.G., King, G.C.P., 2007. Mechanical origin of power law scaling in fault zone rock. Geophys. Res. Lett. 34 (L04312), 1–4.

Savageau, M. A. 1979. Growth of complex systems can be related to the properties of their underlying determinants. Proc. Nat. Acad. Sci. USA. 76, 5413-5417.
Savageau, M. A. 1980. Growth equations: A general equation and a survey of special cases. Mathematical Biosciences48, 267 -278.

Schuhmann, E. V. 1941. Principles of comminution, size distribution and surface calculations. AIME Technical Publication, 1189, 1– 11.
Steacy, S.J., Sammis, C.G.1991. An automaton for fractal patterns of fragmentation. Nature 353, 250-252.
Turcotte, D. L 1986a. A fractal model for crustal deformation. Tectonophysics. 132, 261–269.
Turcotte, D, L. 1986b. Fractals and fragmentation. Journal of Geophysical Research, 91, B2, 1921–1926.
Wolfram Research, Inc., 2021. Mathematica, Version 12.3.1, Champaign, IL.

Weibull, W. 1939. A statistical theory of strength of materials. Proceedings of the Ingeniors Vetenskapsakad, 151.

Figure Captions

Figure 1. Models for fragmentation. (a) The Lienau (1936) one dimensional model. From Grady and Kipp (1985). (b), (c) Two models by Mott and Linfoot (1943) from Grady (2006). (d) Sammis et al, 1987 model. (e) Self similar fracture tree model, from Austin et al. (1972).

Figure 2. The shattering phase transition. Modified from Krapivsky and Ben-Naim (2003) and Phillips and Williams (2021). As the deformation proceeds, the energy of the system is minimised by the simultaneous formation of two phases: coarse grains and dust.

Figure 3. Some processes involved in cataclasite formation. Modified after Phillips and Williams (2021).

Figure 4. Some probability distributions for Phillips et al. (2020, see Phillips and Williams 2021) data. (a) cumulative distribution plot for sample AB2_2. (b) probability plot for sample AB2_2. Pareto Type II followed by Pareto Type I and IV are the best fits. Log-normal is not good. In this and similar figures, the vertical axis for the left hand cumulative distribution plot (a) for each data set is the probability from 0 to 1 and the horizontal axis is the logarithm of the grain size in the units quoted by the authors of the original papers. The right hand figure (b) for each data set is the probability plot with calculated values for the prescribed probability distribution on the vertical axis and measured values on the horizontal axis. The normal distance of the data from the diagonal line on the probability plot (b) is a direct measure of the difference in the goodness of fit.

Figure 5. Log-linear (a) and linear-log models of growth. Variations in the parameter, k, that defines the transition from logarithmic to linear growth (or vice versa) define the type of distribution observed.

Figure 6. Some probability distributions for Phillips et al. (2020) data (Phillips and Williams, 2021) . (a) probability density for sample N_ABB. (b) probability plot for sample N_ABB. Pareto Type I and Type IV are close fits. Pareto Type II is the best fit. Log-normal is not good. (c) and (d) Pareto Type II plotted alone.(e) Raw data, (f) Log-log plot of raw data.

Figure 7. Probability distributions for Melosh et al. (2013) data (Phillips and Williams, 2021). superimposed on fractal interpretations by Melosh et al. (2014, their figure 7A). Frechet2 and Frechet3 are consistently the best fits.

Figure 8. Probability distributions for Hadizadeh et al. (2010) data (Phillips and Williams, 2021). (a) probability density for sample VOF04A. (b) probability plot for sample VOF04A. Gamma4 and Pareto4 are the best fits.

Figure 9. Some probability distributions for Fagereng (2011) data (Phillips and Williams, 2021). (a) probability density for sample GM_CB14. (b) probability plot for sample GM_CB14. Frechet2 and Frechet3 are the best fits.

Figure 10. Some probability distributions for Blenkinsop (1991) data. (a) Probability density for sample 6181.3HX20. (b) Probability plot for sample 6181.3HX20. Generalised Gamma, GompertzM4 and Gumbel2 are good fits. Logistic2 is not as good as the other three.

Figure 11. Some probability distributions for Marone and Scholtz (1979) data (Phillips and Williams, 2021). (a) probability density for sample 04_c. (b) probability plot for sample 04_c. Fréchet2 and Generalised Gamma are good fits (c) probability density for sample 05_c. (d) probability plot for sample 05_c. Fréchet2 is best fit followed closely by Generalised Gamma.

Figure 12. Best fit probability distributions from Ferreira and Coop (2020) data.

Figure 13. Some fits of various distributions for Montheil et al. (2020) data (Tonalite high mag x400). Best fits are Fréchet2, Fréchet3 and Pareto Type IV.

Figure 14. Comparison of Generalised Gamma and Gompertz fits for data set 6241.3NX20X of Blenkinsop (1991). The Generalised Gamma distribution is to be expected from theory and we label it a *fundamental distribution*. The Gompertz distribution is not predicted by existing theory and we label it an *incidental distribution*. In fact the Gompertz distribution under-estimates the data at the coarsest of grain sizes.

Figure 15. Decrease in fragmentation frequency with decrease in fragment size. This is consistent with a self similar fragmentation rate where fragmentation decreases with fragment size. Modified from Marone and Scholtz (1989). It is also consistent with the proposals of Einav (2007 a, b; Nguyen and Einav, 2009) that the elastic energy responsible for driving fragmentation decreases as the fragment size decreases.

Tables

Table 1. Kinetics of fragmentation (Cheng and Redner, 1990; Redner, 1990). λ is the homogeneity index and is a measure of the rate of fragmentation, $r \sim x^{\lambda}$. The symbols b_1, υ, c_2 are various parameters defined in Cheng and Redner, (1990).

Model	Description of process	Probability distribution function	Probability distribution	Comments
Linear fragmentation, $\lambda > 0$ Larger grains more likely to break	Breakage due to externally applied loads, no collisional breakage.	$\phi(x) \sim x^{b_1-2}\, exp(-ax^{\lambda});\; x \to \infty$ $\phi(x) \sim exp\left(-\frac{\lambda}{2\, ln\, x_0}(ln\, x)^2\right);\; x \to 0$ $\phi(x) \sim x^{\upsilon} \quad ; x \to 0$	Generalised gamma Log-normal Power law	True for large fragments Fragmentation with a lower cut-off for breakage. Fragmentation down to small sizes
Linear fragmentation, $\lambda < 0$ Smaller grains more likely to break	Shattering transition	Theoretically all grains infinitely small. Shattering begins immediately as deformation begins. $\phi(x) \sim x^{-(1+\lambda)}$.	Power law	All grains very small. Probability distribution said to be Power law in natural materials.
Collision induced fragmentation Model I $\lambda \geq 1$	Both particles split upon collision	$\phi(x) \sim x^{-2}\, exp\left(-x^{\frac{\lambda}{2}}\right);\; x \to \infty$ $\phi(x) \sim exp\left(-\frac{\lambda}{4\, ln\, 2}(ln^2\, x)\right);\; x \to 0$	Gamma Log-normal	Coarse grained Fine grained
Collision induced fragmentation	Larger particles split upon collision	$\phi(x) \sim x^{-2}\, exp\left(-x^{\frac{\lambda}{2}}\right); x \to \infty$ $\phi(x) \sim exp\left(-\frac{c_2}{x}\right);\; x \to 0$	Gamma	Coarse grained

Model II $\lambda \geq 1$			Exponential	Fine grained
Collision induced fragmentation Model III $\lambda \geq 1$	Smaller particles split upon collision	$\phi(x) \sim x^{-(1+\lambda)};\quad x \to \infty$ $\phi(x) \sim exp\left(-\frac{\lambda}{2\, ln\, 2}(ln^2\, x)\right);\ x \to 0$	Power law Log-normal	Coarse grained Fine grained
Collision induced fragmentation $\lambda < 1$	Shattering transition at $\lambda = 1$	Shattering transition is a continuous ("second order") phase transition so that the energy of the system is minimised by the simultaneous development of coarse and dust phases (Krapivsky and Ben-Naim, 2003; Krapivsky et al., 2017).	No information available on grain size distributions in natural materials.	No information available on grain size distributions in natural materials.

Table 2. Common probability distributions involved in fragmentation. y is fragment size. The other symbols express the position, scale, shape, mean, mode and standard deviation of the distributions and are not necessarily related to other or identical symbols in this paper.

Distribution	**Probability density function, *F*(*x*)**	**Graphical representation of cumulative distribution**	**Scaling Relation***
Fréchet/ Weibull	$\frac{\alpha}{s}\left(\frac{y-m}{s}\right)^{-1-\alpha}\exp\left[-\left(\frac{y-m}{s}\right)^{-\alpha}\right]$ $\frac{k}{\lambda}\left(\frac{y}{s}\right)^{k-1}\exp\left[-\left(\frac{y}{\lambda}\right)^{k}\right]$	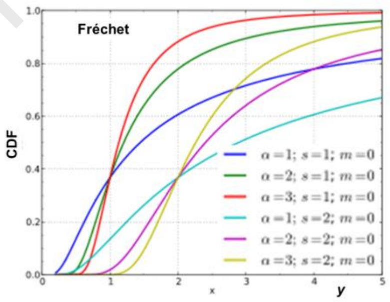 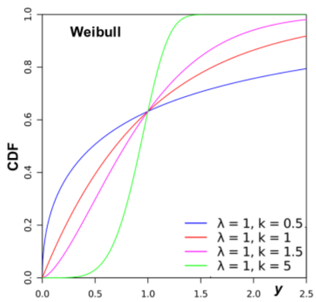	Logarithmic
Exponential	$\lambda\exp(-\lambda y)$	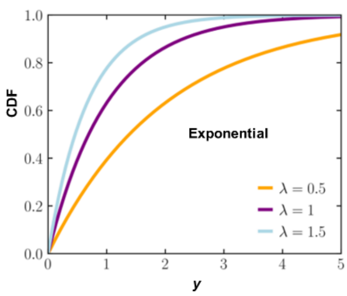	

Gamma	$$\frac{y^{k-1}}{\Gamma(k)\theta^k}\exp\left(-\frac{y}{\theta}\right)$$	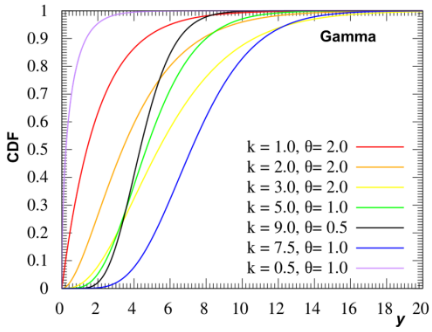	Logarithmic Linear
Gauss/ Normal	$$\frac{1}{\sigma\sqrt{2\pi}}\exp\left[-\frac{1}{2}\left(\frac{y-\mu}{\sigma}\right)^2\right]$$	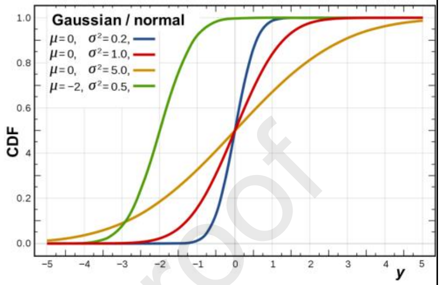	Linear
Generalised gamma Also known as gamma4	$$\frac{p/a^d}{\Gamma(d/p)}y^{d-1}\exp\left[(-y/a)^p\right]$$	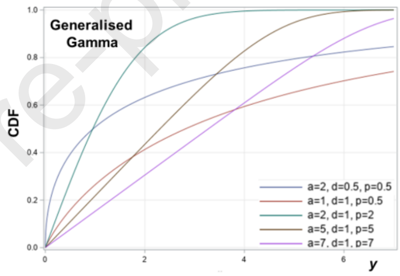	Logarithmic Linear
Gumbel	$$\frac{1}{\beta}\exp\left[-\left(z+\exp(-z)\right)\right]$$ where $$z=\frac{y-\mu}{\beta}$$	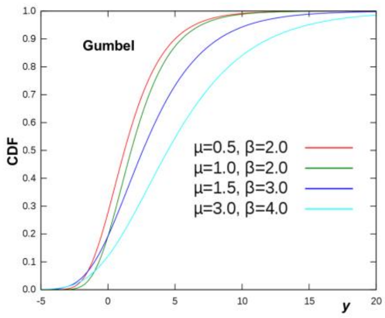	Linear
Log-normal	$$\frac{1}{y\sigma\sqrt{2\pi}}\exp\left(-\frac{(\ln y-\mu)^2}{2\sigma^2}\right)$$	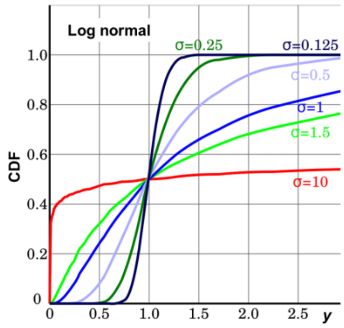	Linear
Generalised Pareto family. See Arnold (1983),	ParetoDistribution[k,α] ParetoDistribution[k,α,μ] ParetoDistribution[k,1,γ,μ]	Pareto2 Pareto Type I Pareto3 Pareto Type II Pareto Type III	

Pareto typ
Pareto typ
Pareto typ

Pickards (1975).	ParetoDistribution[k,α,γ,μ]	Pareto4 Pareto Type IV		Pareto typ
Pareto Type I (Power-law)	$\frac{\alpha y_m^{\alpha}}{y^{\alpha+1}}$	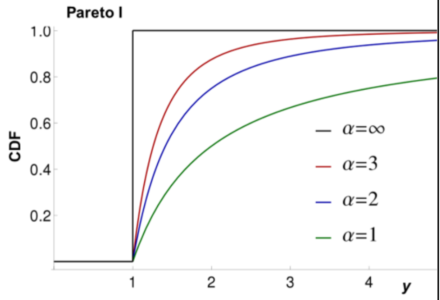	Logarithmic	
Pareto Type II (Lomax) The Pareto II is a Pareto I shifted to the left	$\frac{\alpha}{\lambda}\left(1+\frac{y}{\lambda}\right)^{-(\alpha+1)}$	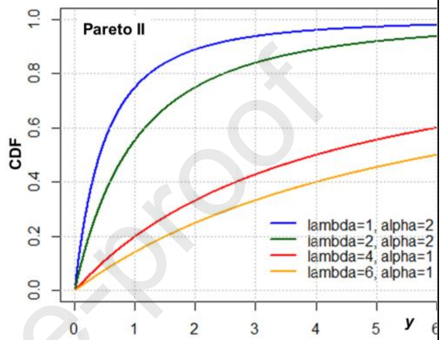	Logarithmic	
Pareto Types III and IV (Type III corresponds to $\alpha = 1$)	$\left[1+\left(\frac{y-\mu}{\sigma}\right)^{\frac{1}{\gamma}}\right]^{-\alpha}$	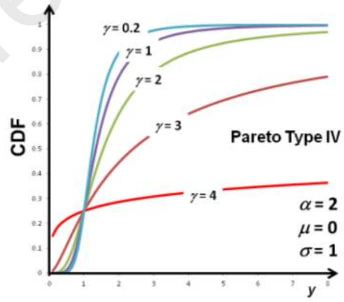	Logarithmic	
Gompertz	$b\eta \exp\left[\eta + by - \eta \exp(by)\right]$ The GompertzMakeham distribution is a four parameter Gompertz distribution.	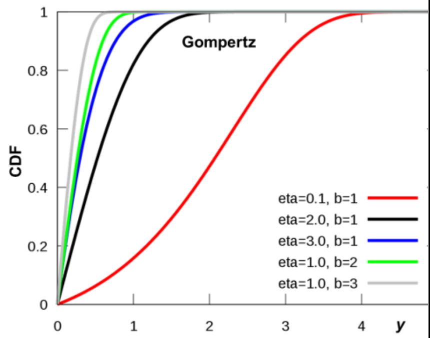	Linear	

*Table modified from Frank (2014; Table 1). All graphics for distributions except Generalised Gamma distributions and Pareto 3 and 4 modified from Wikipedia. Generalised Gamma distributions modified from https://blogs.sas.com/content/iml/2021/03/15/generalized-gamma-distribution.html. Pareto IV calculated by present authors.

Table 3. Calculated values of the homogeneity index, λ, from some Generalised Gamma distributions.

Data set	Homogeneity index, λ.
Blenkinsop	

1582.0H#36X20	2.98
1582.0H #37 X20	2.78
1712.1AE1X20	7.27
1724.1HX20	12.60
1724.5NX20	4.50
2298.7HX20#21	2.88
2298.7HX20#22	35595.9
2298.7HX20#23	2.84
2298.7HX20#23R	2.87
2298.7HX20#24	2.90
2301EX20	3.05
Fagereng	
GM_CB14	3.18
Phillips+Williams	
AB2_2	7.13
AB2F	3.80
AB2SB	7.21
AB3	4.37
AB3S	6.03
AB3U	4.77
N_ABB	4.31
N_ABF	4.40
N_SM	4.01
SM2	3.46
SM2I	3.27
SM3A	5.73
SM3I	5.31
SM3W	4.25
Montheil et al.	
graniteHiMag x1600	0

Appendix. Best fit distributions.

In this appendix we present the best fit distributions for each data set. The detailed distributions are presented in Supplementary Material. The data for Fagereng (2011), Hadizadeh et al. (2010), Marone and Scholz (1989), Melosh et al. (2014) and Phillips et al. (2020) were downloaded from the repository described by Phillips & Williams (2021), Acknowledgments, Samples, and Data, of 10 .17605 /OSF.IO /JDW8N

Table A1. Best fit distributions for Phillips and Williams (2021) data.

Phillips and Williams (2021)			
SAMPLE	**Probability Distribution #1**	**Probability Distribution #2**	**Probability Distribution #3**
AB2_2	Pareto type II	Pareto type IV; Weibull3; Gamma4	Frechet3
AB2F	Pareto type II	Pareto type IV; Weibull3; Gamma4	Frechet3
AB2SB	Pareto type II	Pareto type IV; Weibull3; Gamma4	Frechet3

AB3	Pareto type II	Pareto type IV; Weibull3; Gamma4	Frechet3
AB3S	Pareto type II		
AB3U	Pareto type II		
N_ABB	Pareto type II		
N_ABF	Pareto type II		
N_SM	Pareto type II		
SM2	Pareto type II		
SM2A	Pareto type II		
SM2I	Pareto type II		
SM3A	Pareto type II		
SM3I	Pareto type II		
SM3W	Pareto type II		

Table A2. Best fit distributions for Melosh et al. (2014) data.

Melosh et al 2014				
SAMPLE		Probability Distribution #1	Probability Distribution #2	Probability Distribution #3
PS126	chaotic	Pareto type IV	Frechet3	Frechet2
PS194A		Frechet3	Pareto type IV/Gamma4	InverseGaussian
PS194b	crackle breccia	Frechet3/Frechet2	Pareto type II/InverseGaussian	Weibull3
PS195	chaotic	Frechet2	Frechet3	Pareto type IV
PS197		Frechet3	Frechet2	Gamma4/LogNormal/InverseGaussian
PS204	crackle breccia	Frechet3	Frechet2	
PSKB	crackle breccia	Frechet3	Pareto type II/Gamma4	Weibull3
PSON	crackle breccia	Frechet3	Weibull3/Gamma4	Pareto type II

Table A3. Best fit distributions for Hadizadeh. (2010) data.

Hadizadeh. (2010)			
SAMPLE	**Probability Distribution #1**	**Probability Distribution #2**	**Probability Distribution #3**
VOF01	Pareto type IV	Gamma4	Frechet3
VOF01DMZN	Gamma4	Weibull3	Pareto type IV
VOF03A	Gamma4	Weibull3	Pareto type IV
VOF04A	Gamma4	Pareto type IV	Frechet3
VOF04DMZN	Weibull3/Pareto type II	Pareto type IV/Gamma4	Frechet2
VOF05AB	Pareto type IV	Gamma4	Frechet3
VOF07	Pareto type IV	Frechet3	Gamma4/LogNormal

Table A4. Best fit distributions for Fagereng (2011) data.

Fagereng (2011) melange

SAMPLE	Probability Distribution #1	Probability Distribution #1	Probability Distribution #1
GM_CB1	Pareto type IV	Frechet3	Frechet2
GM_CB11	Pareto type II	Frechet3/Pareto type I	Frechet2
GM_CB12_XY	Pareto type IV	Frechet3	Frechet2
GM_CB12_XZ	Frechet3		
GM_CB12_YZ	Frechet3		
GM_CB12_ZX_Thin	Frechet3		
GM_CB12_ZY_thin	Frechet3		
GM_CB14	Frechet3	Frechet2	Pareto type II
GM_CB15_Fold	Frechet3	Frechet2	Pareto4
GM_CB15_XZ	Frechet3	Pareto4	Frechet2

Table A5. Best fit distributions for Blenkinsop (1991) data.

Blenkinsop (1991)			
SAMPLE	Probability Distribution #1	Probability Distribution #2	Probability Distribution #3
1582.0H#36	GompertzMakeham4/Gumbel2	Gamma4	
1582.0H#37	GompertzMakeham4	Gumbel2	Gamma4
1712.1AE1	GompertzMakeham4/Gumbel2/Gamma4		
1724.1H	GompertzMakeham4/Gumbel2/Gamma4		
1724.1H	GompertzMakeham4/Gumbel2/Gamma4		
1724.1H	GompertzMakeham4	Gumbel2	
1724.5N	GompertzMakeham4/Gumbel2/Gamma4		
2298.7H#21	GompertzMakeham4/Gumbel2	Gamma4	
2298.7H#22	Gamma4	Gumbel2	
2298.7H#22R	GompertzMakeham4/Gumbel2	Gamma4	
2298.7H#23	GompertzMakeham4/Gumbel2	Gamma4	
2298.7H#23R	GompertzMakeham4/Gumbel2	Gamma4	
2298.7H#24	GompertzMakeham4/Gumbel2	Gamma4	
2301E	GompertzMakeham4/Gumbel2	Gamma4	
2301EX20RR	GompertzMakeham4/Gumbel2	Gamma4	
3359.3H	GompertzMakeham4/Gumbel2	Gamma4	
4442.9A#22	No Data		
4442.9A#23	No Data		
4442.9A#23R	No Data		
5437.5AE#24	GompertzMakeham4/Gumbel2	Gamma4	
5437.5AE#24R	repeat		
6181.3H	Gumbel2/Gamma4		
6181.3HXX	GompertzMakeham4/Gumbel2/Gamma4		
6241.3E	Gumbel2/Gamma4	GompertzMakeham4	Gamma4
6241.3NX	GompertzMakeham4/Gumbel2/Gamma4		
7381.4N	Gamma4	GompertzMakeham4/Gumbel2	
9206.0H#30	GompertzMakeham4/Gumbel2	Gamma4	
9206.0H#31	GompertzMakeham4/Gumbel2	Gamma4	

Table A6. Best fit distributions for Marone and Scholtz (1979) data

Marone & Scholz (1979)			
SAMPLE	Probability distribution #1	Probability Distribution #2	Probability distribution #3
04_C	Pareto type II	Pareto type IV/Weibull3/Frechet3	Frechet3/Frechet2
05C	Pareto type II	Pareto type IV/Weibull3/Frechet3	Frechet2
07C	Pareto type II		
34100	Pareto type II		
37100	Pareto type II		
A04C	Pareto type II		
A00C	Pareto type II		
GSA01C	Pareto type II		
GS11C	Pareto type II		

Table A7. Best fit distributions for Ferreira and Coop (2020) data.

Ferreira and Coop (2020)	Probability distribution #1	Probability distribution #2	Probability distribution #3
Shear Strain %			
440	Pareto type II	Fréchet2	Fréchet3
6940	Pareto type I	Pareto type II	Gamma4
44500	Gamma4	Pareto type I	Fréchet3

Table A8. Best fit distributions for Montheil et al. (2020) data.

Montheil et al., 2020		Magnification	Distribution #1	Distribution #2	Distribution #3
Granite	High	x400	Fréchet3	Pareto type II	Pareto type I
		x800			
		x1600	Fréchet3	Gamma4	
	Low	x100	Fréchet3	Fréchet2	Pareto type IV
		x200			
		x400	Pareto type IV	Fréchet3	Fréchet2
Tonalite	High	x400	Fréchet3	Fréchet2	Pareto type IV
		x800			
		x1600	Fréchet3	Fréchet2	Pareto type IV
	Low	x100	Fréchet2	Fréchet3	Pareto type IV
		x200			
		x400	Fréchet3	Pareto type IV	Gamma4

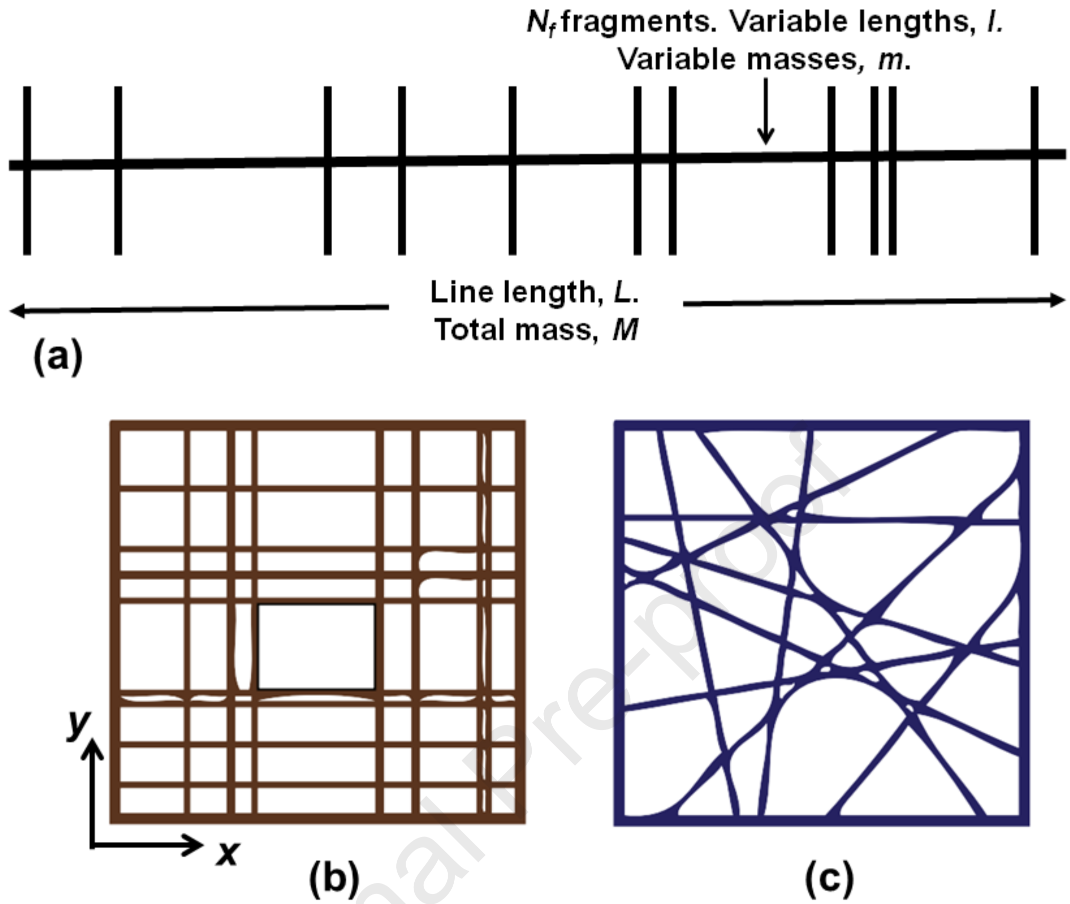
N_f fragments. Variable lengths, l.
Variable masses, m.
Line length, L.
Total mass, M
(a)
y
x
(b)
(c)

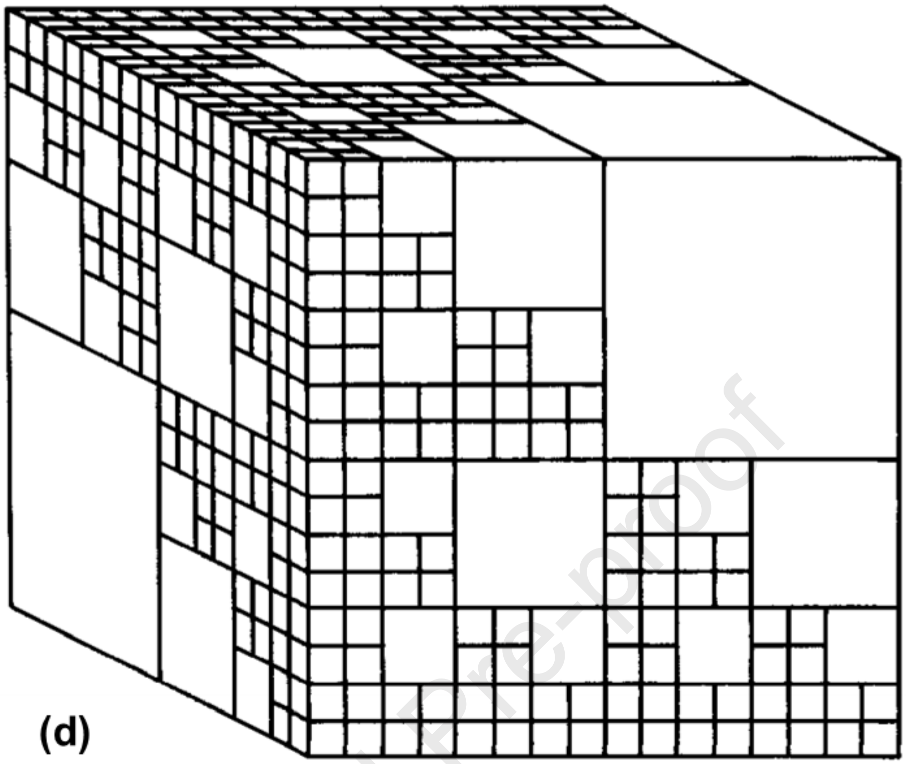

(d)

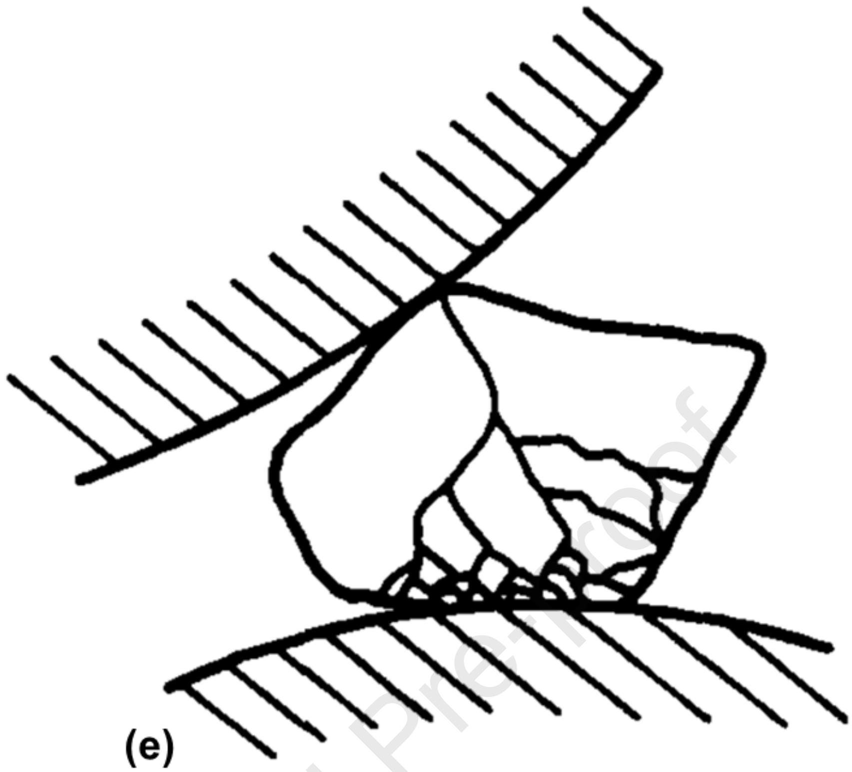

(e)

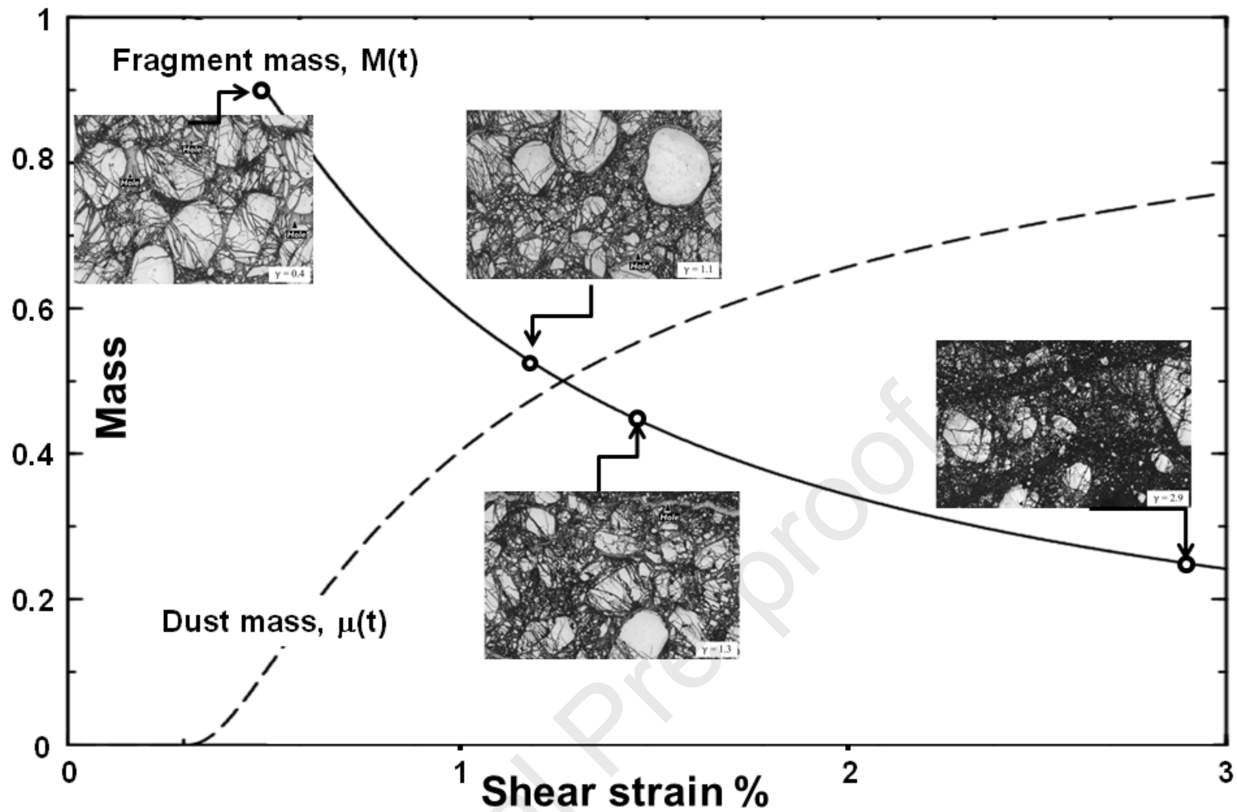
Fragment mass, M(t)
Dust mass, μ(t)
Mass
Shear strain %
0
0.2
0.4
0.6
0.8
1
0
1
2
3

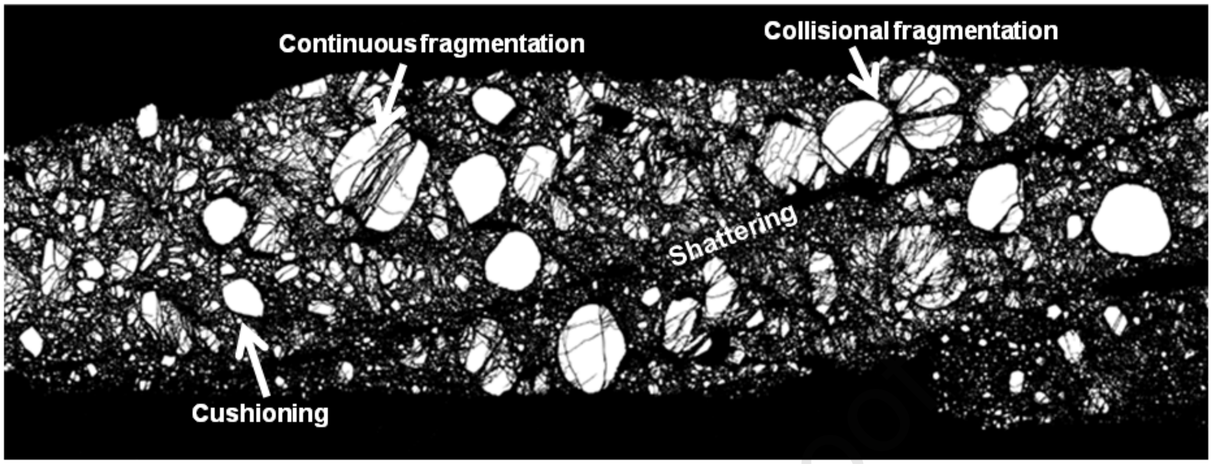
Continuous fragmentation
Collisional fragmentation
Shattering
Cushioning

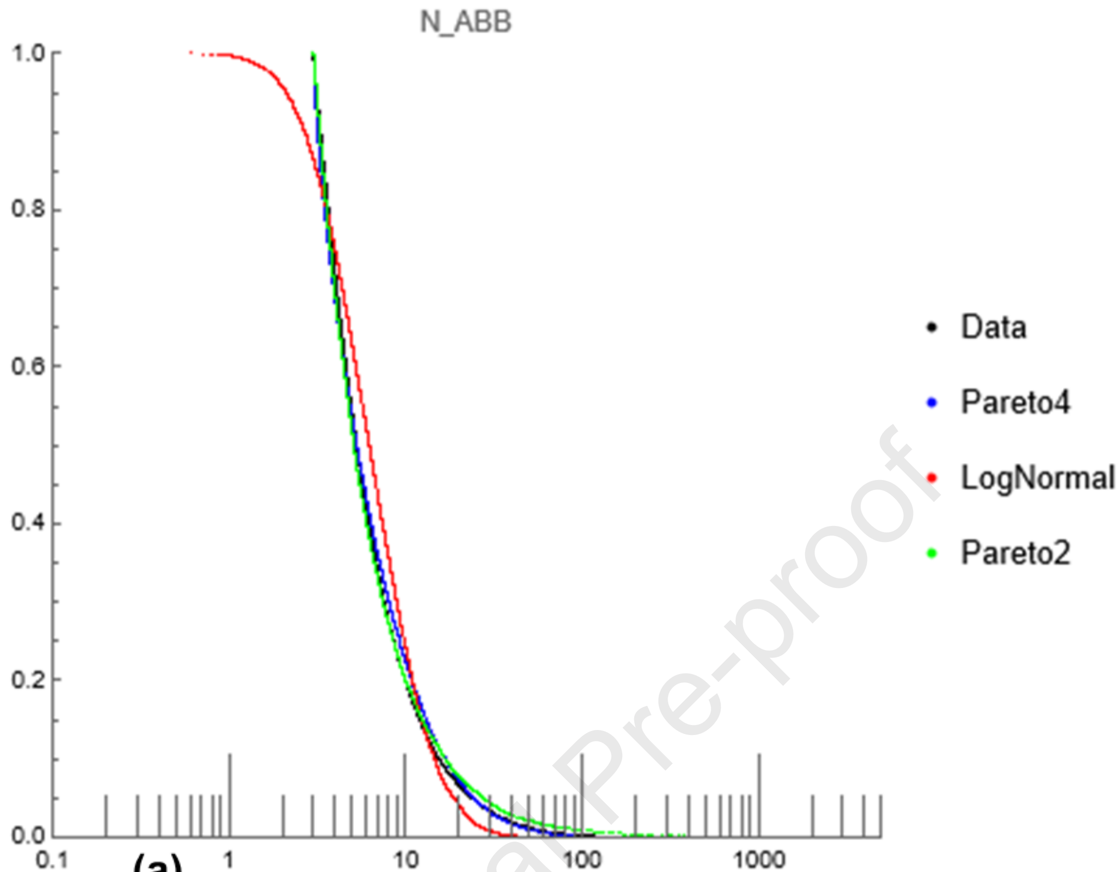
N_ABB
1.0
0.8
0.6
0.4
0.2
0.0
0.1
1
10
100
1000
Data
Pareto4
LogNormal
Pareto2

(a)

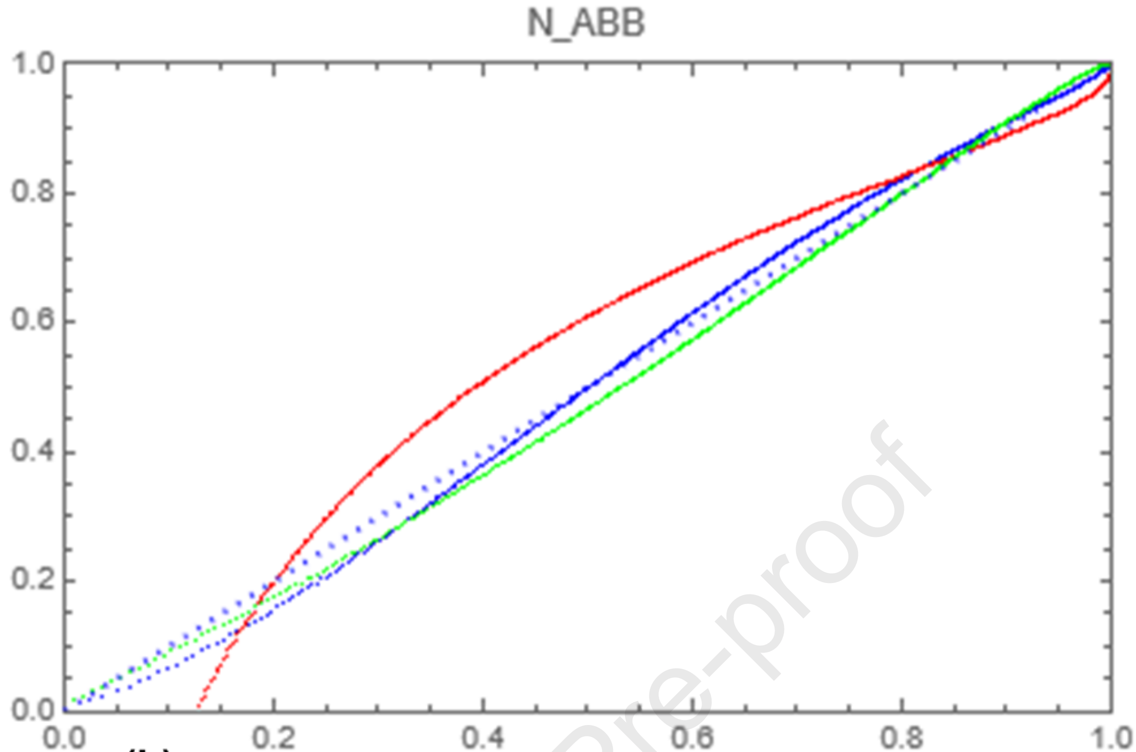

(b)

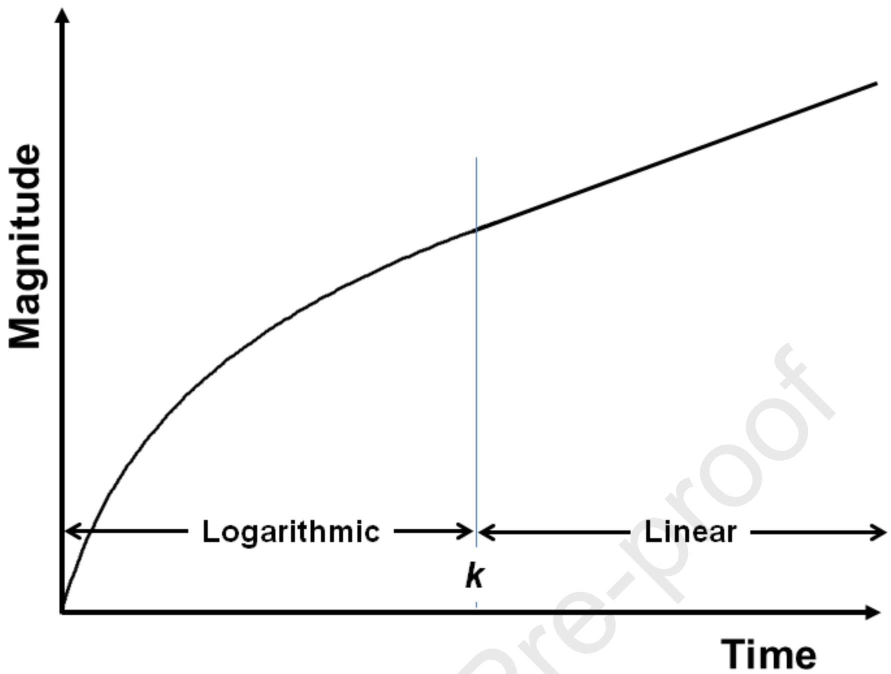

(a)

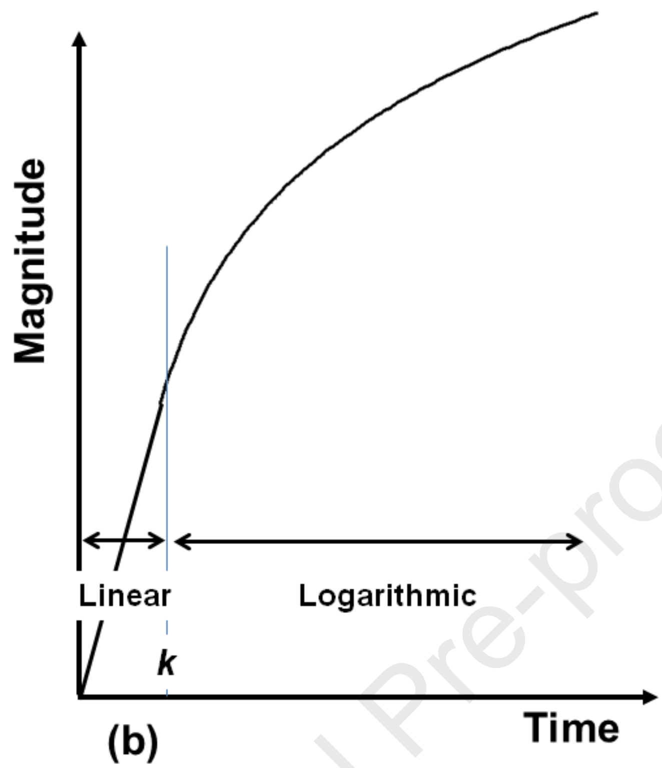
Magnitude
Linear
Logarithmic
k
(b)
Time

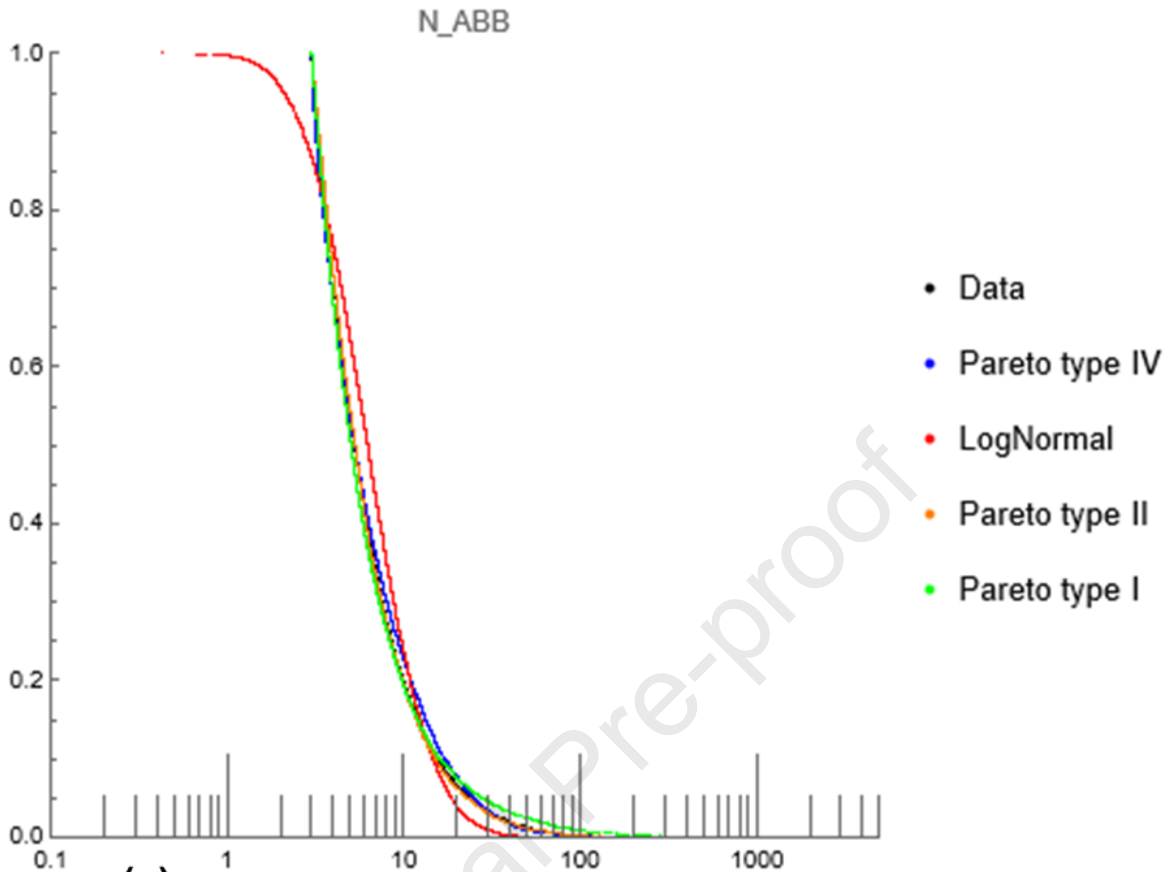

N_ABB
1.0
0.8
0.6
0.4
0.2
0.0
0.1
1
10
100
1000
Data
Pareto type IV
LogNormal
Pareto type II
Pareto type I

(a)

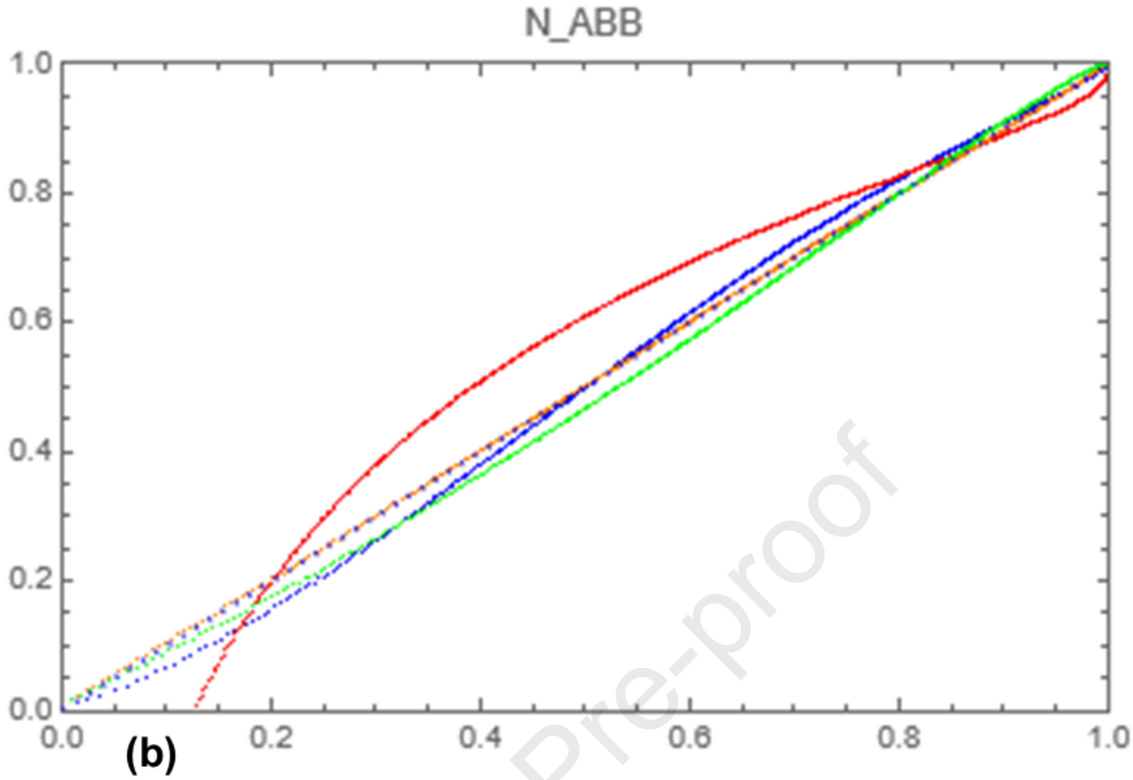
N_ABB
1.0
0.8
0.6
0.4
0.2
0.0
0.0
0.2
0.4
0.6
0.8
1.0
(b)

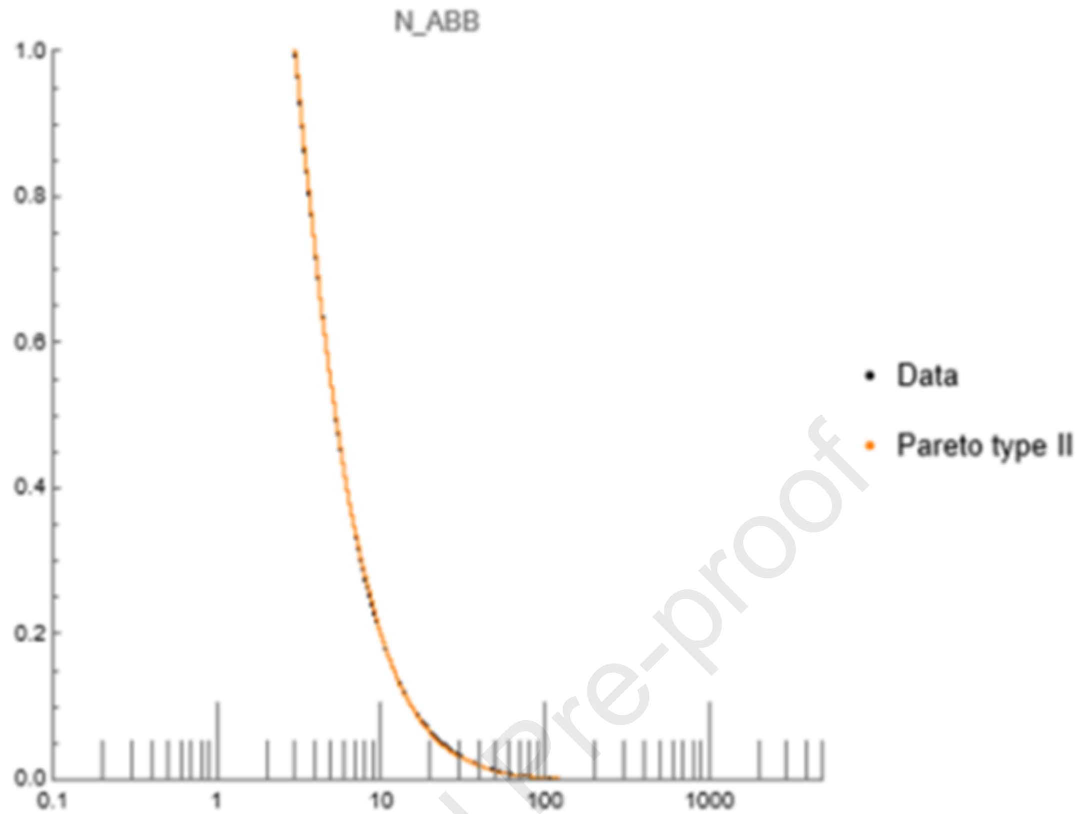

(c)

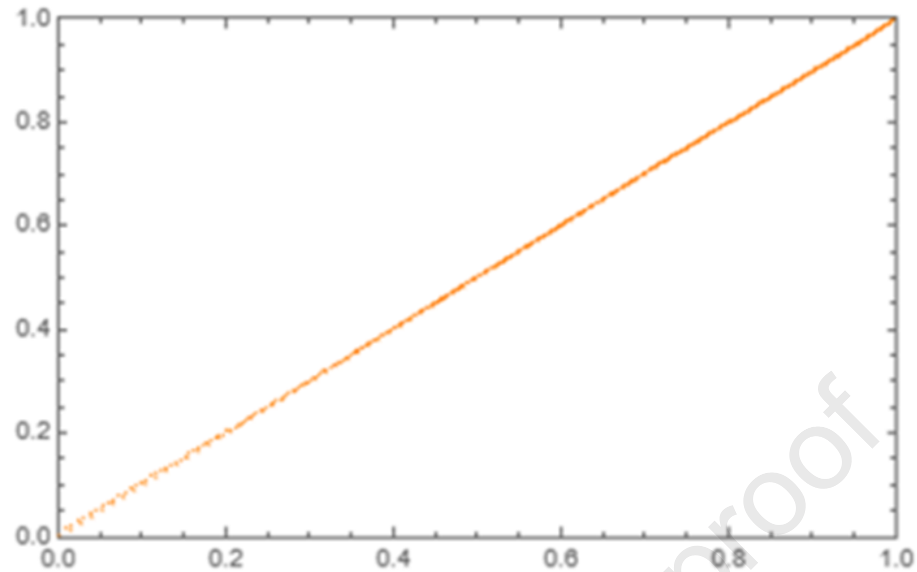

(d)

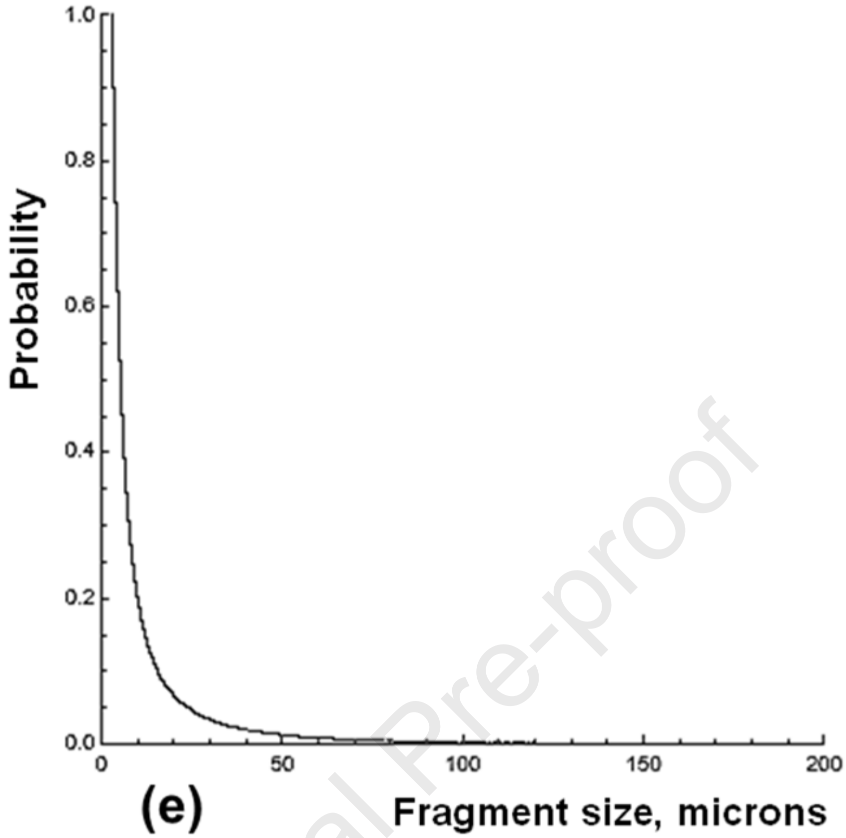
Probability
1.0
0.8
0.6
0.4
0.2
0.0
0
50
100
150
200
Fragment size, microns

(e)

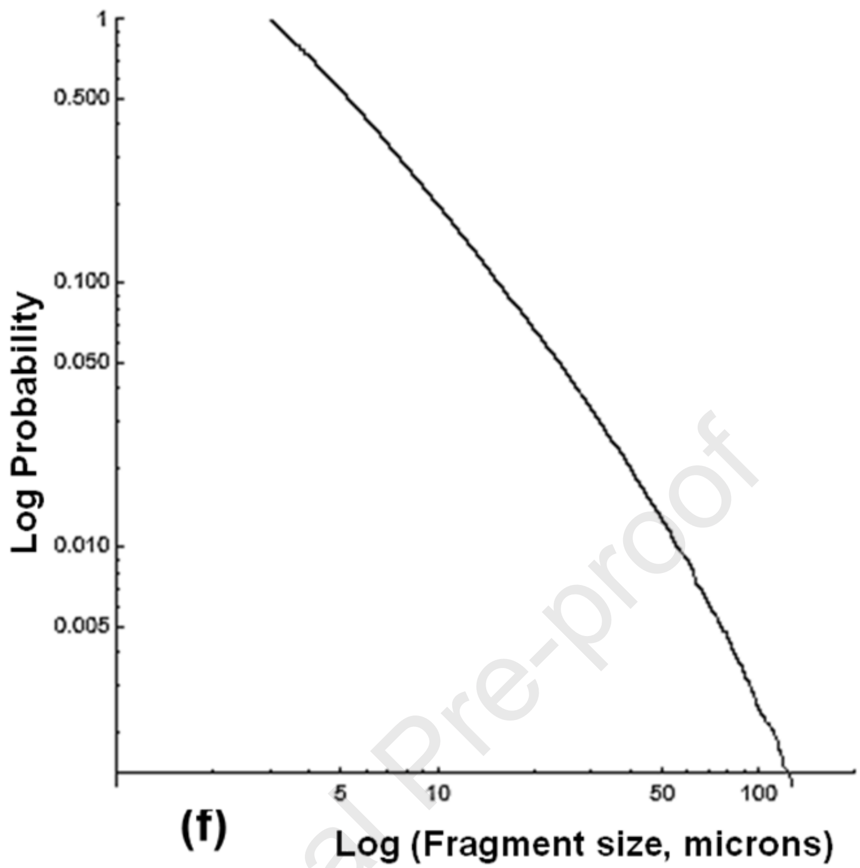

Log Probability
1
0.500
0.100
0.050
0.010
0.005
5
10
50
100
(f)
Log (Fragment size, microns)

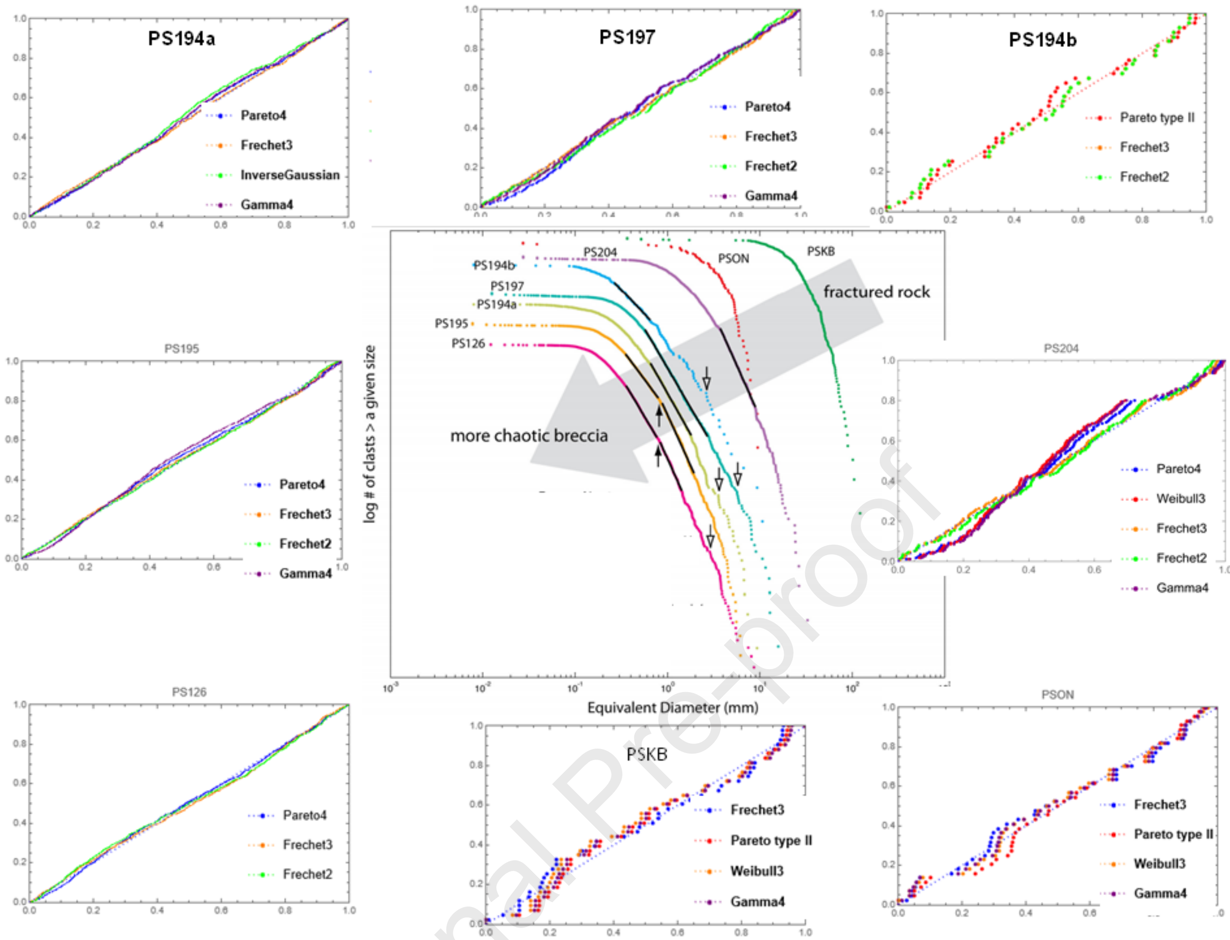

PS194a
Pareto4
Frechet3
InverseGaussian
Gamma4
PS197
Pareto4
Frechet3
Frechet2
Gamma4
PS194b
Pareto type II
Frechet3
Frechet2
PS195
Pareto4
Frechet3
Frechet2
Gamma4
PS204
Pareto4
Weibull3
Frechet3
Frechet2
Gamma4
PS126
Pareto4
Frechet3
Frechet2
PSKB
Frechet3
Pareto type II
Weibull3
Gamma4
PSON
Frechet3
Pareto type II
Weibull3
Gamma4
PS204
PSON
PSKB
PS194b
PS197
PS194a
PS195
PS126
fractured rock
more chaotic breccia
log # of clasts > a given size
Equivalent Diameter (mm)

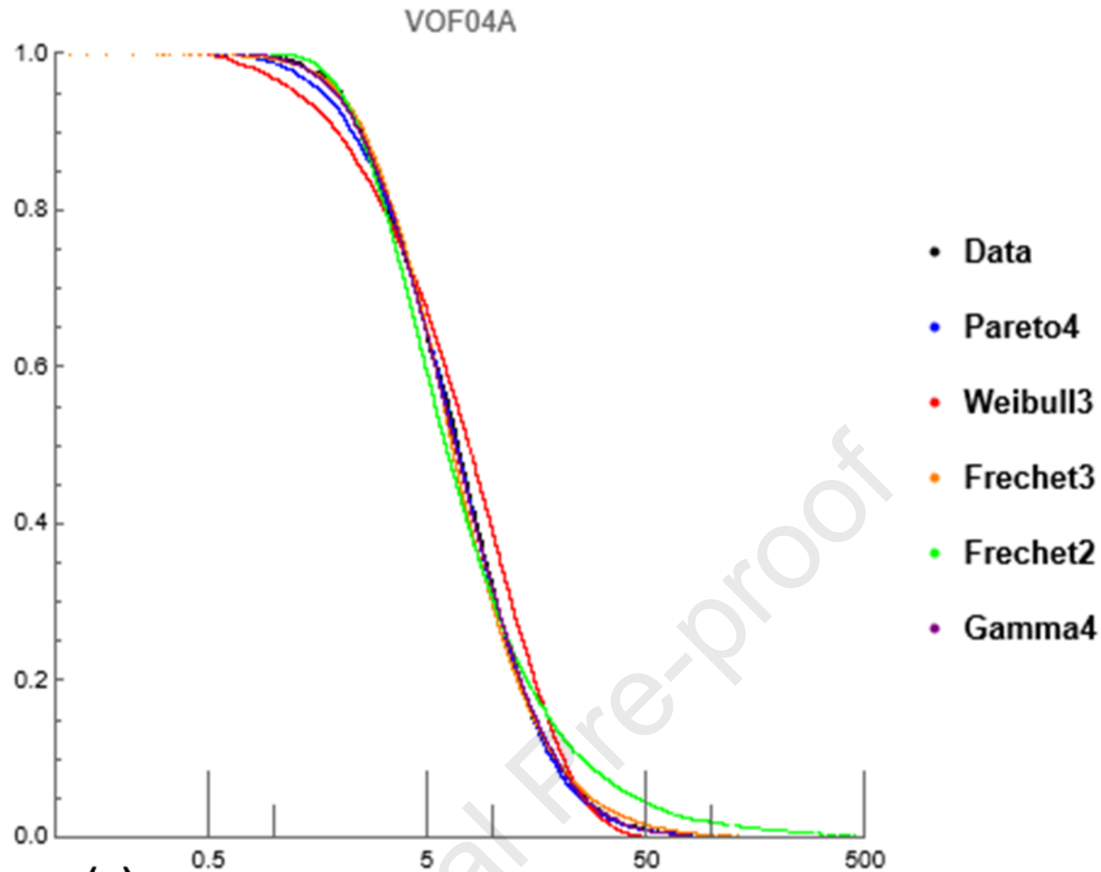
VOF04A
1.0
0.8
0.6
0.4
0.2
0.0
0.5
5
50
500
Data
Pareto4
Weibull3
Frechet3
Frechet2
Gamma4

(a)

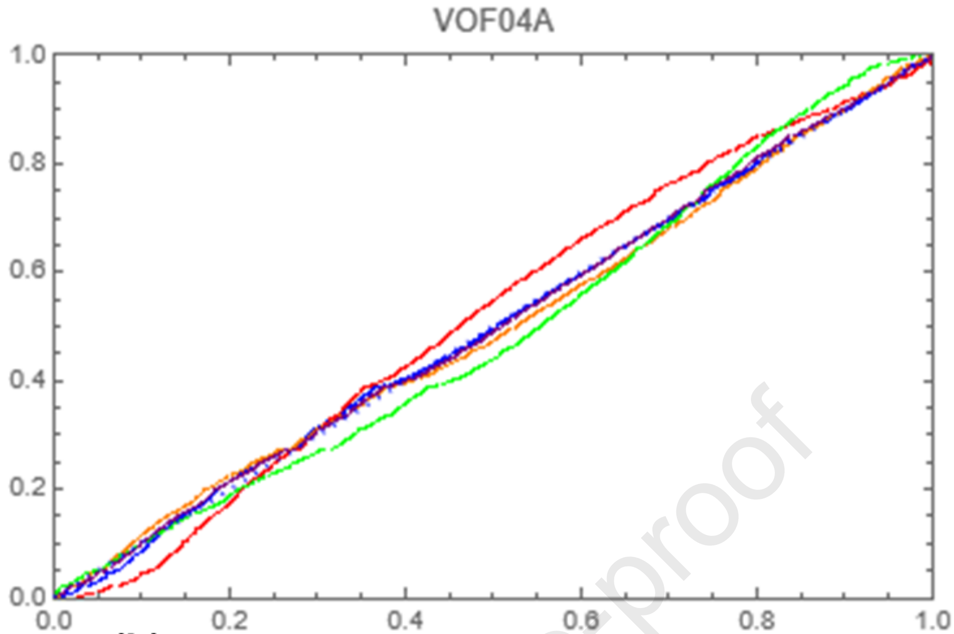

(b)

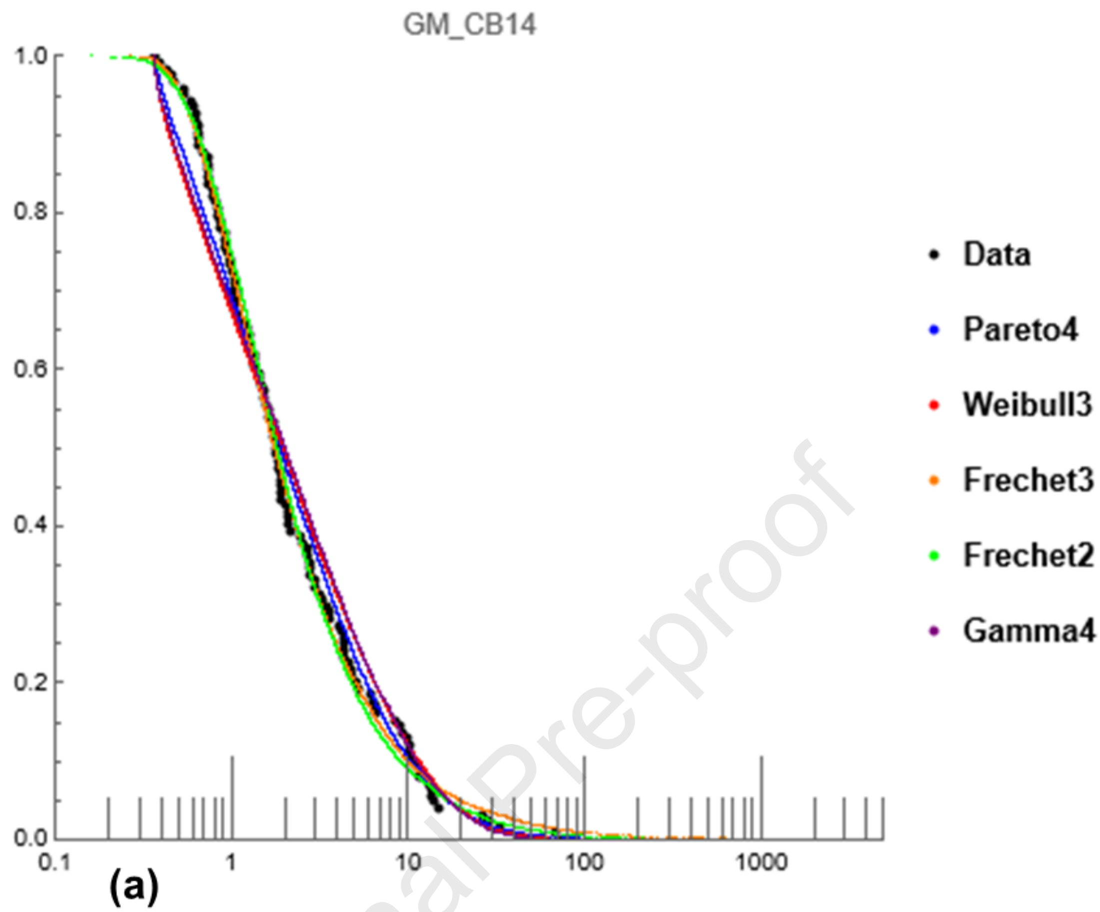
GM_CB14
1.0
0.8
0.6
0.4
0.2
0.0
0.1
1
10
100
1000
Data
Pareto4
Weibull3
Frechet3
Frechet2
Gamma4
(a)

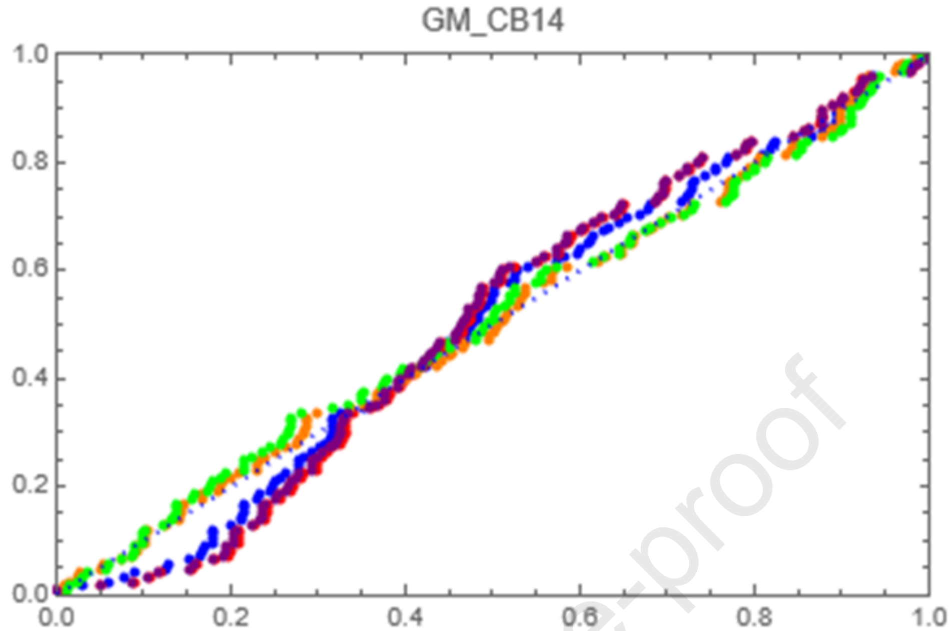

(b)

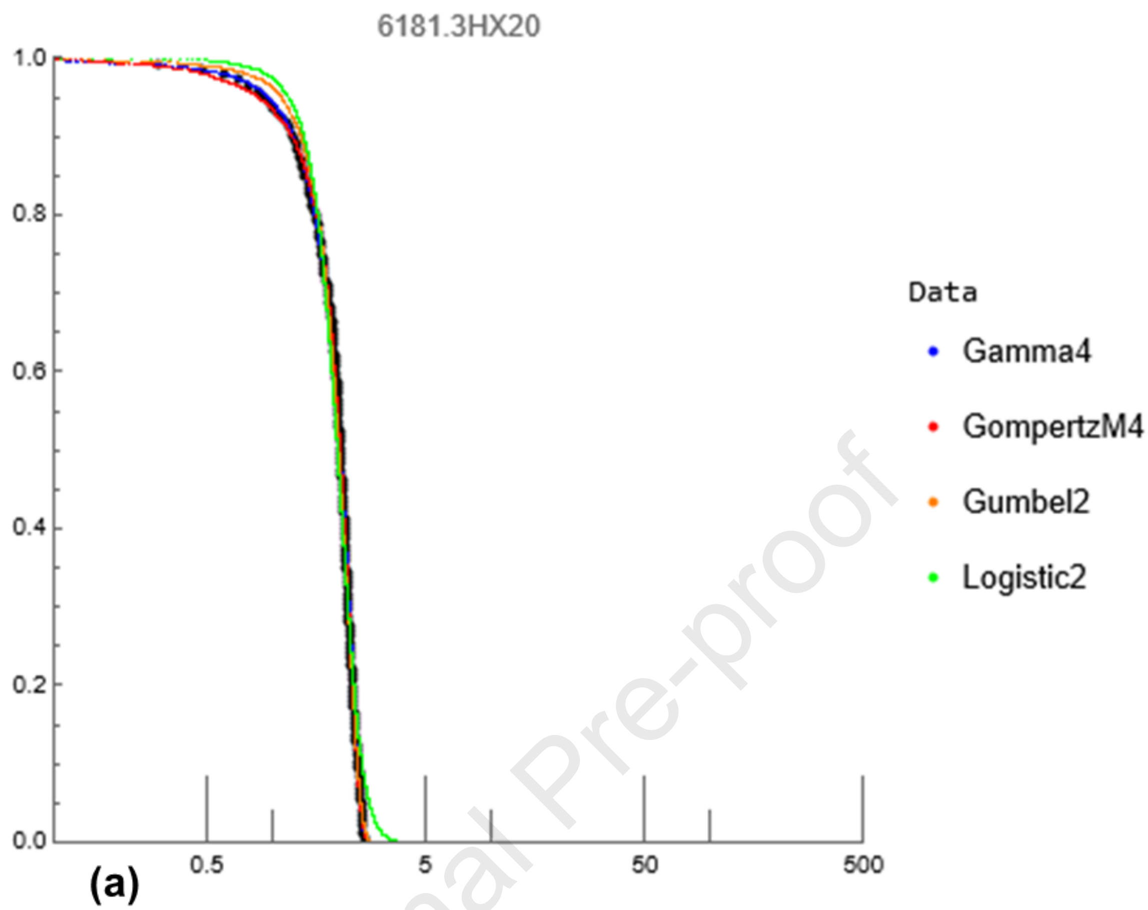
6181.3HX20
1.0
0.8
0.6
0.4
0.2
0.0
0.5
5
50
500
(a)
Data
Gamma4
GompertzM4
Gumbel2
Logistic2

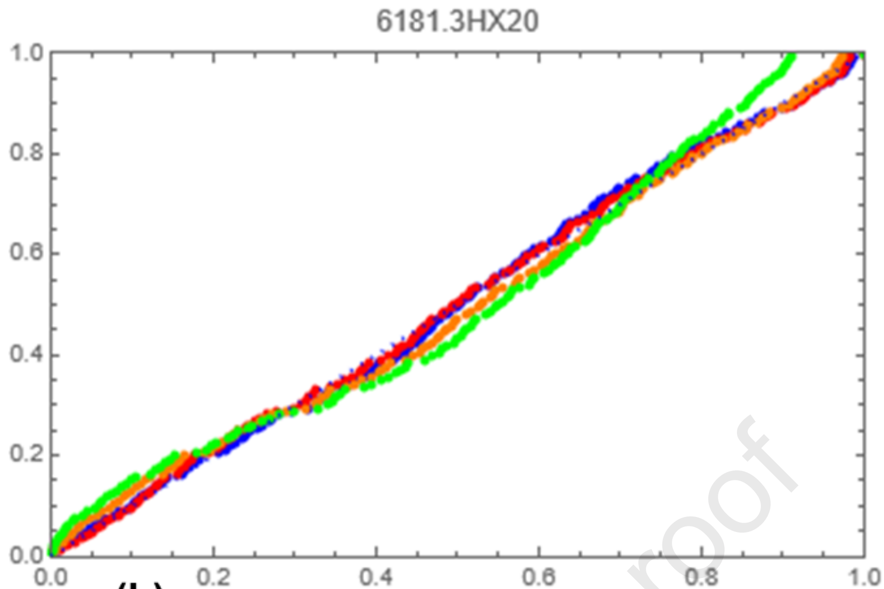

(b)

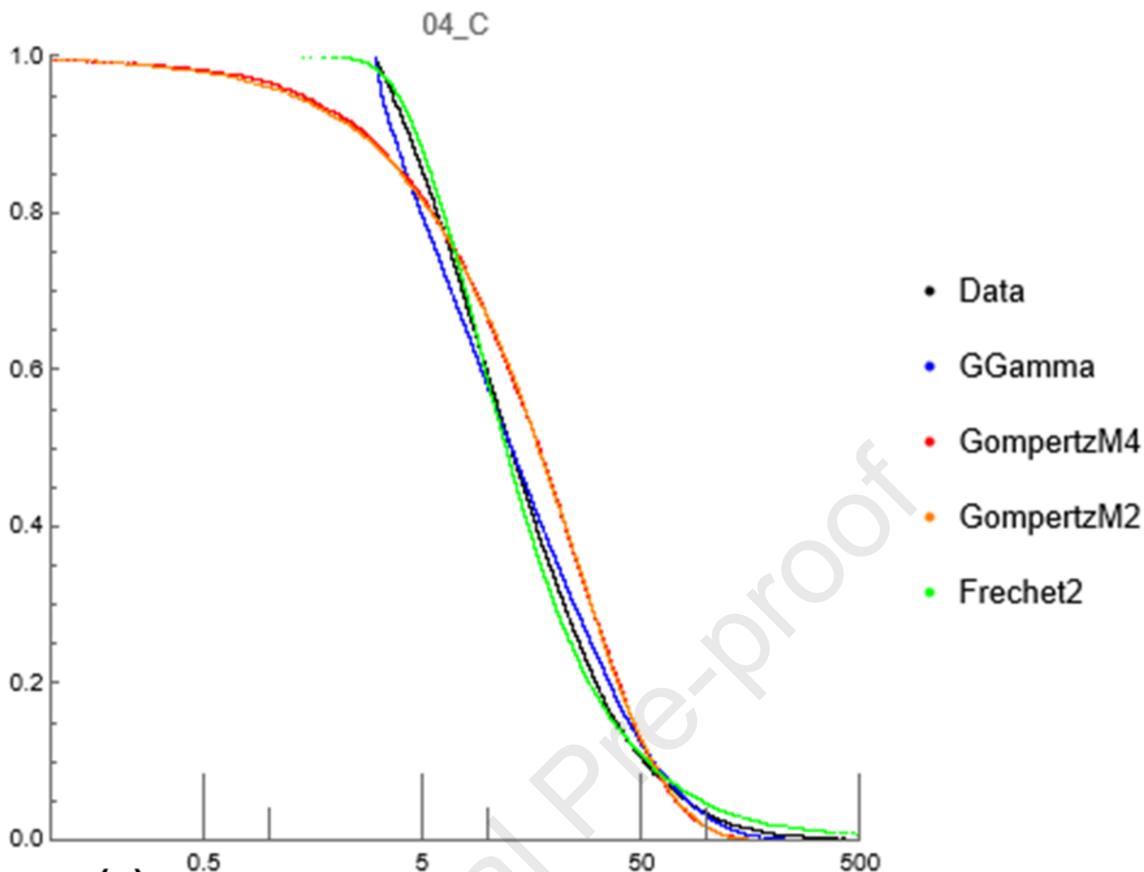
04_C
1.0
0.8
0.6
0.4
0.2
0.0
0.5
5
50
500
Data
GGamma
GompertzM4
GompertzM2
Frechet2

(a)

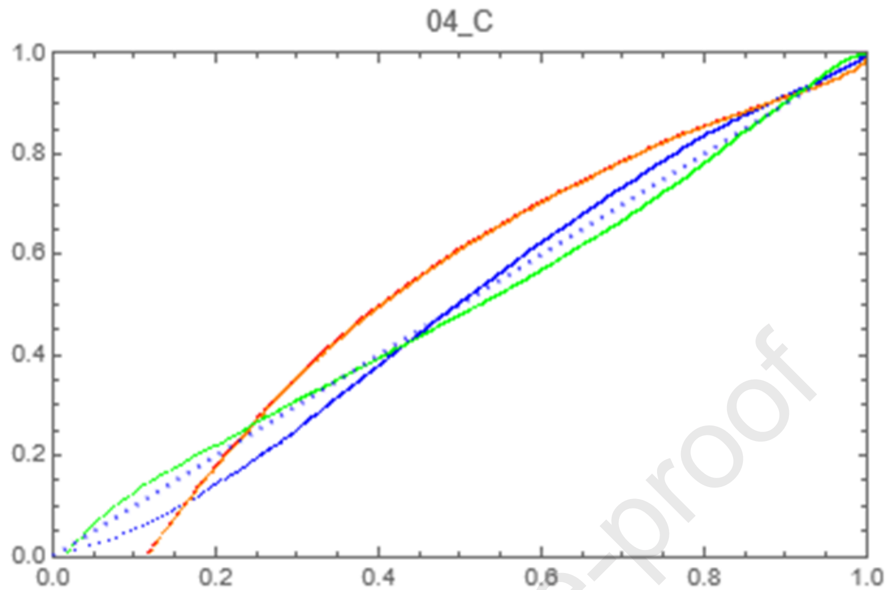

(b)

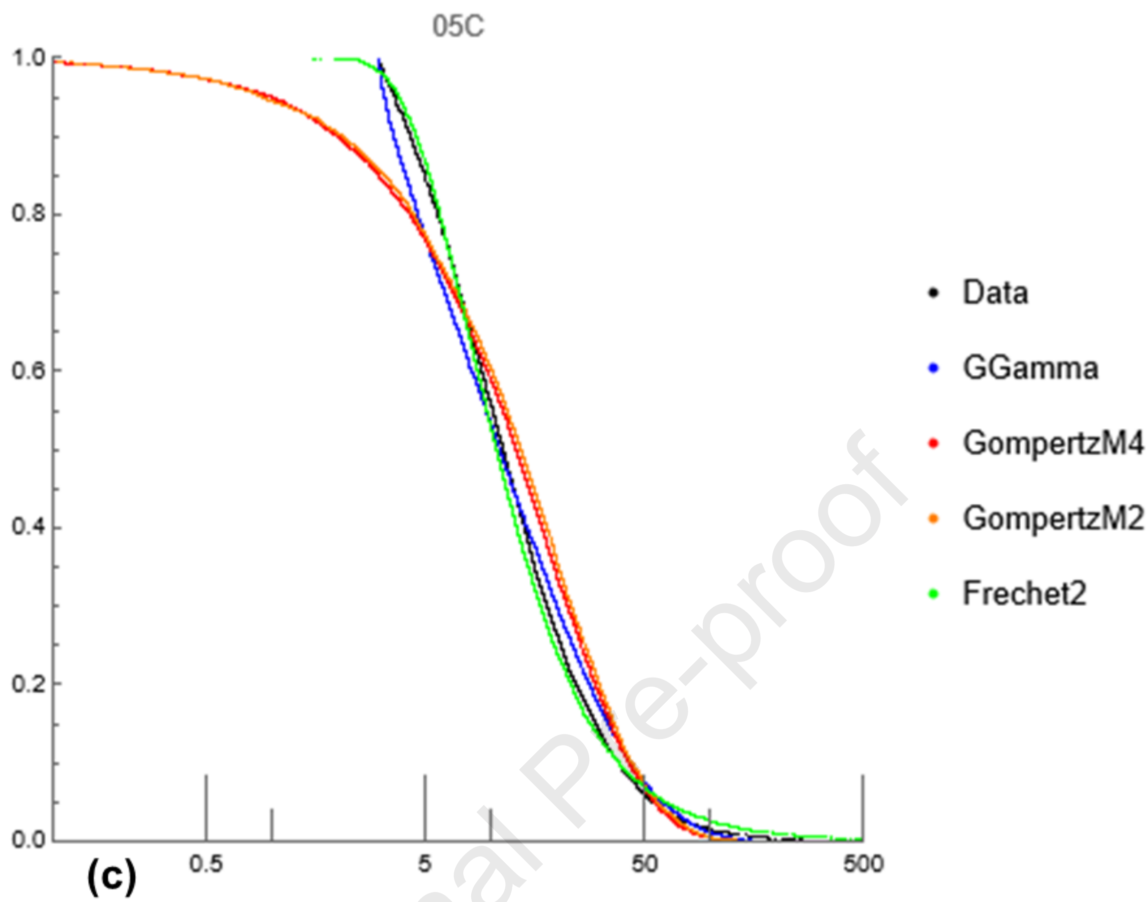
05C
1.0
0.8
0.6
0.4
0.2
0.0
0.5
5
50
500
Data
GGamma
GompertzM4
GompertzM2
Frechet2
(c)

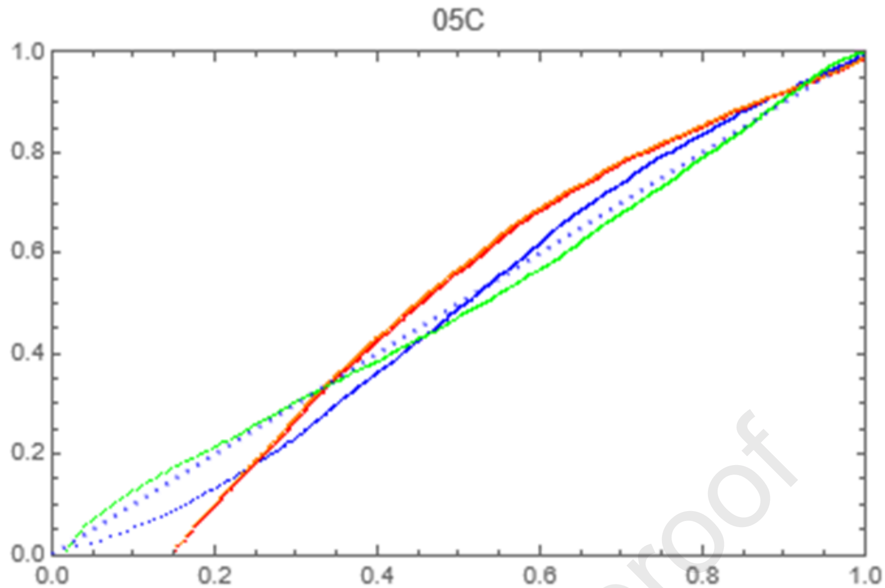

(d)

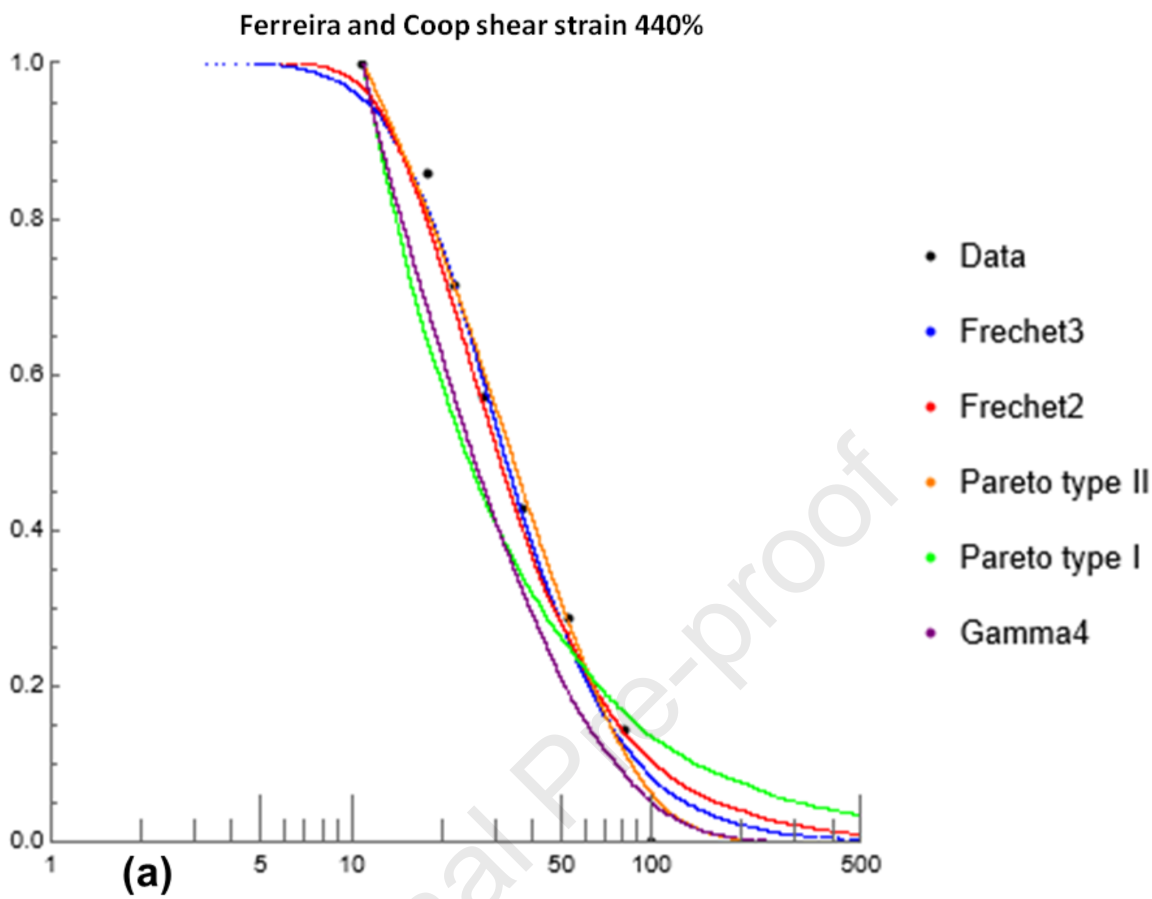

Ferreira and Coop shear strain 440%
1.0
0.8
0.6
0.4
0.2
0.0
1
5
10
50
100
500
(a)
Data
Frechet3
Frechet2
Pareto type II
Pareto type I
Gamma4

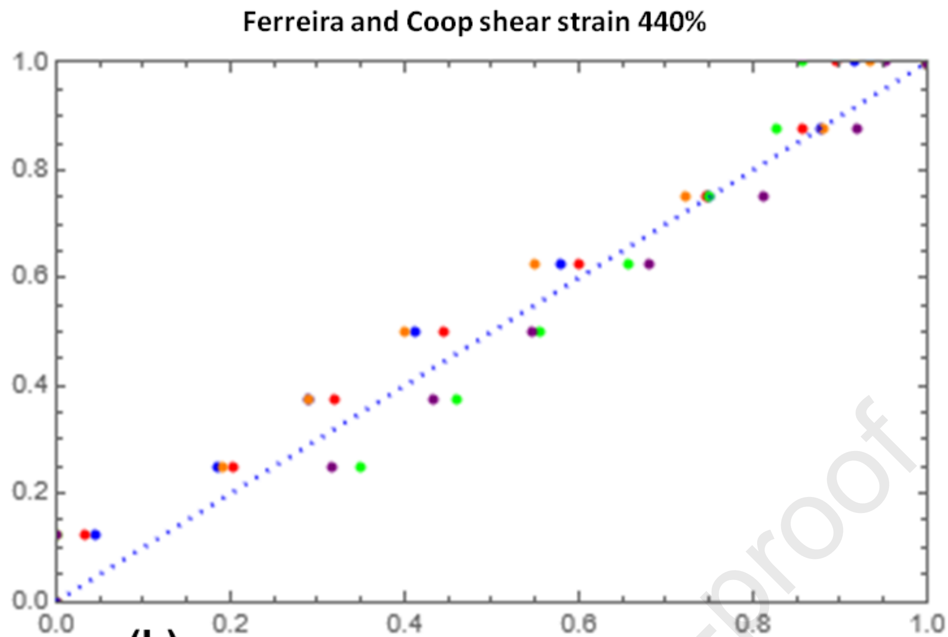
Ferreira and Coop shear strain 440%
1.0
0.8
0.6
0.4
0.2
0.0
0.0
0.2
0.4
0.6
0.8
1.0

(b)

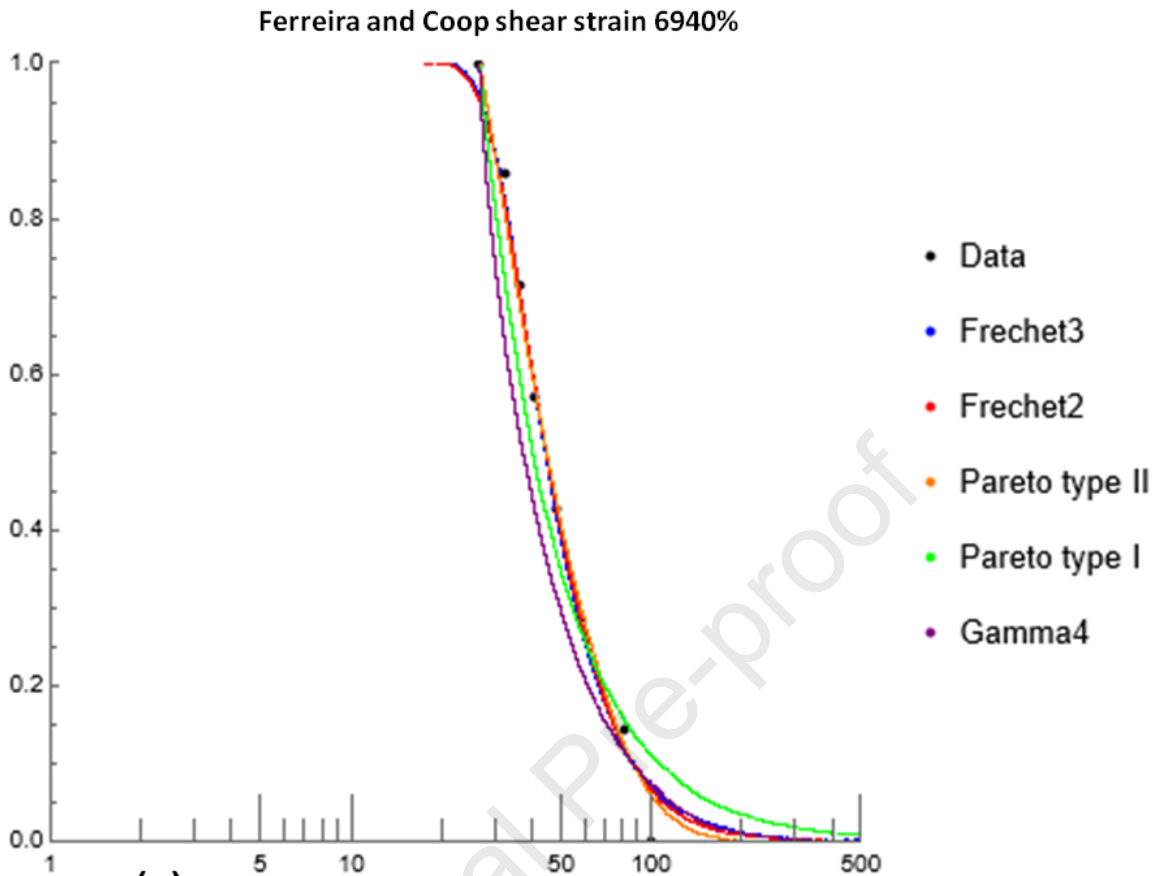
Ferreira and Coop shear strain 6940%
1.0
0.8
0.6
0.4
0.2
0.0
1
5
10
50
100
500
Data
Frechet3
Frechet2
Pareto type II
Pareto type I
Gamma4

(c)

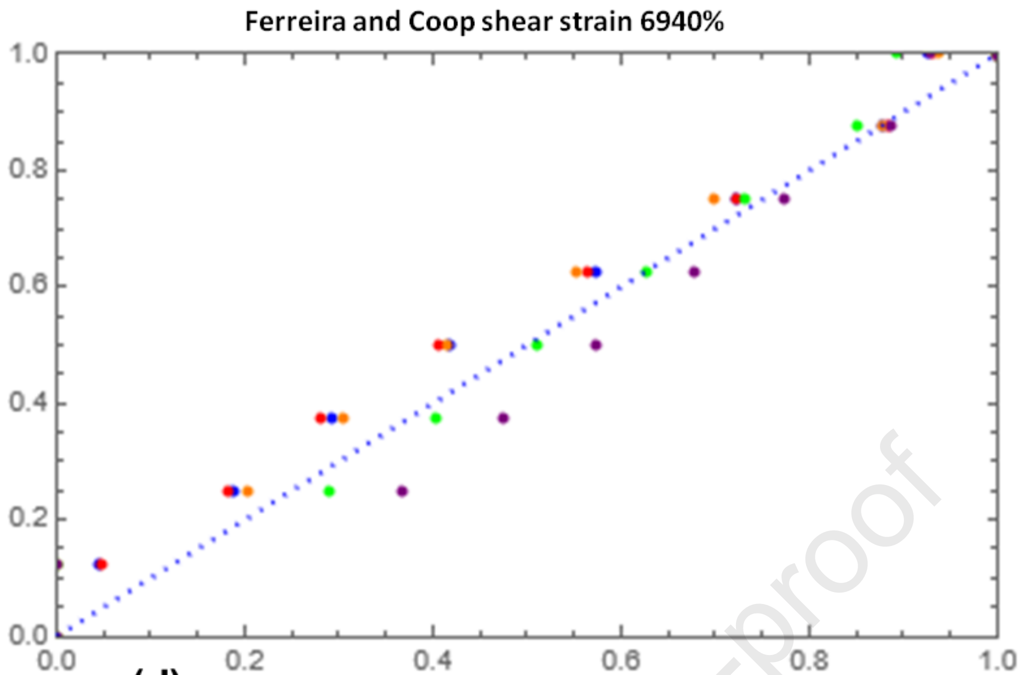
Ferreira and Coop shear strain 6940%
1.0
0.8
0.6
0.4
0.2
0.0
0.0
0.2
0.4
0.6
0.8
1.0

(d)

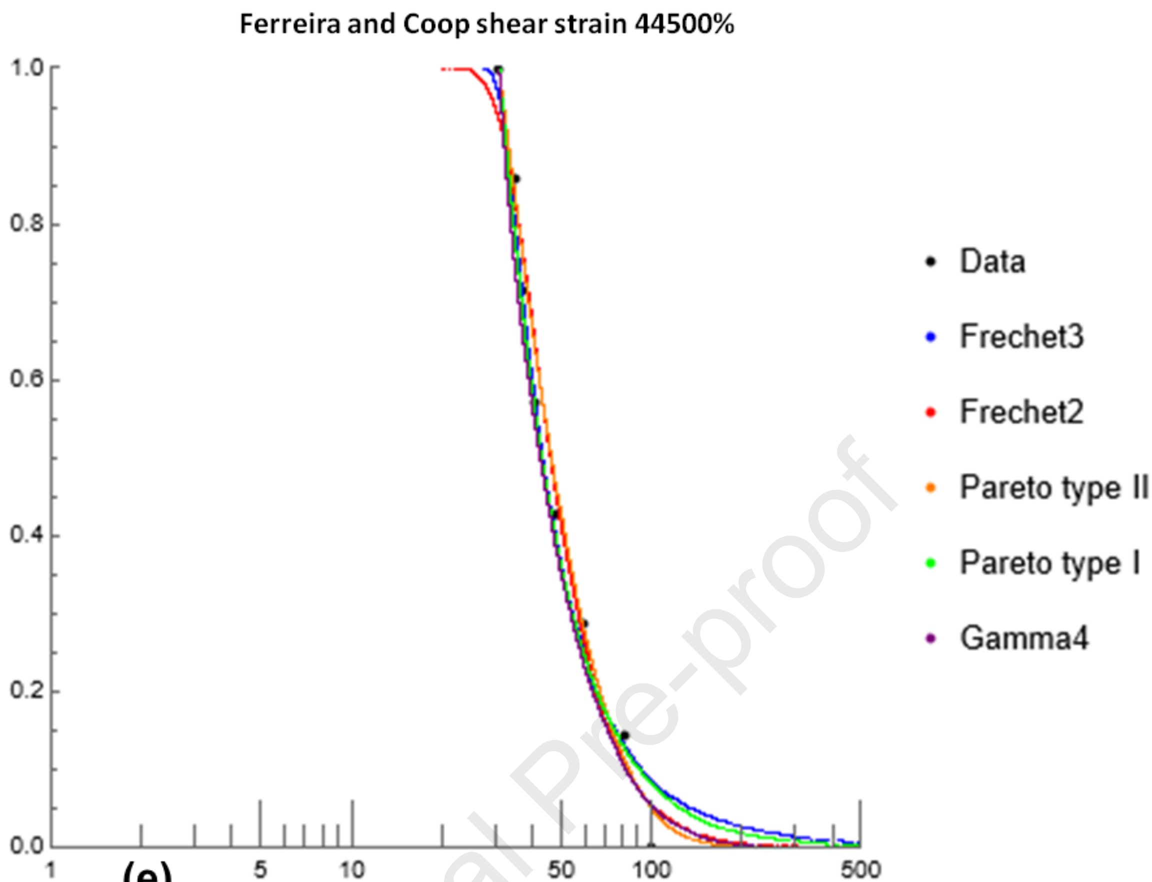
Ferreira and Coop shear strain 44500%
1.0
0.8
0.6
0.4
0.2
0.0
1
5
10
50
100
500
Data
Frechet3
Frechet2
Pareto type II
Pareto type I
Gamma4

(e)

Ferreira and Coop shear strain 44500%

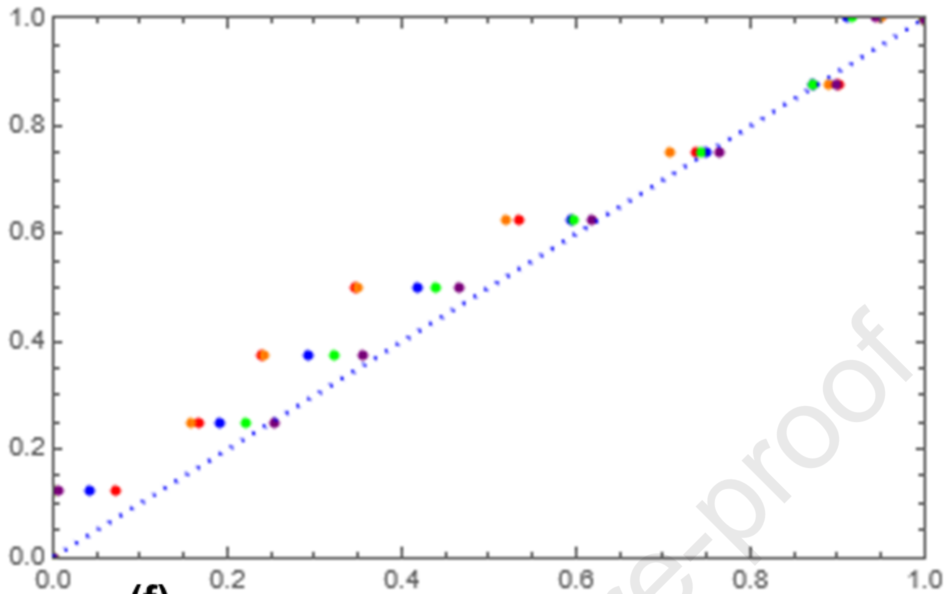

(f)

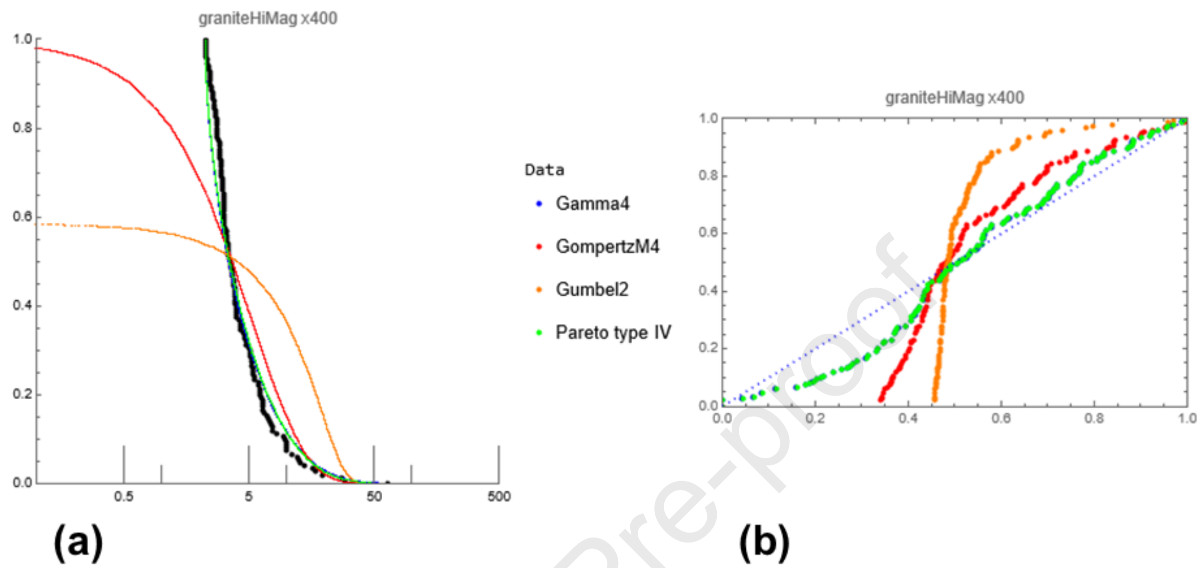
graniteHiMag x400
1.0
0.8
0.6
0.4
0.2
0.0
0.5
5
50
500
Data
Gamma4
GompertzM4
Gumbel2
Pareto type IV
graniteHiMag x400
1.0
0.8
0.6
0.4
0.2
0.0
0.0
0.2
0.4
0.6
0.8
1.0
(a)
(b)

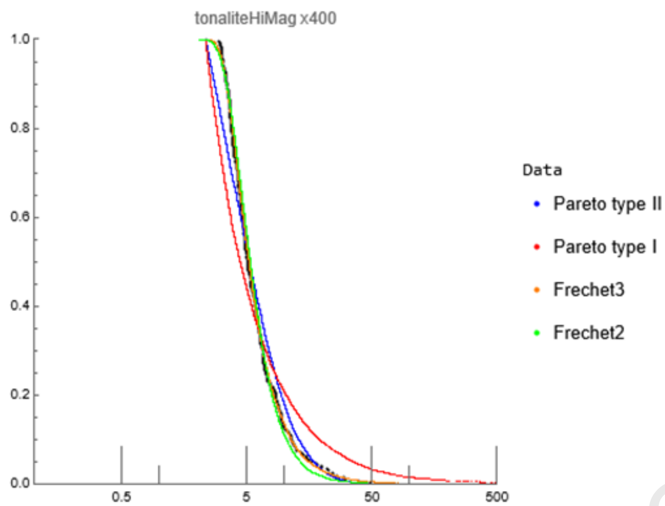
tonaliteHiMag x400
1.0
0.8
0.6
0.4
0.2
0.0
0.5
5
50
500
Data
Pareto type II
Pareto type I
Frechet3
Frechet2

(c)

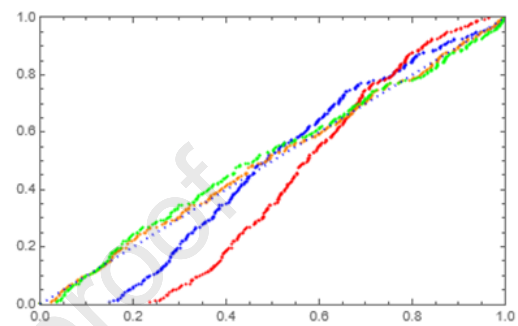
1.0
0.8
0.6
0.4
0.2
0.0
0.0
0.2
0.4
0.6
0.8
1.0

(d)

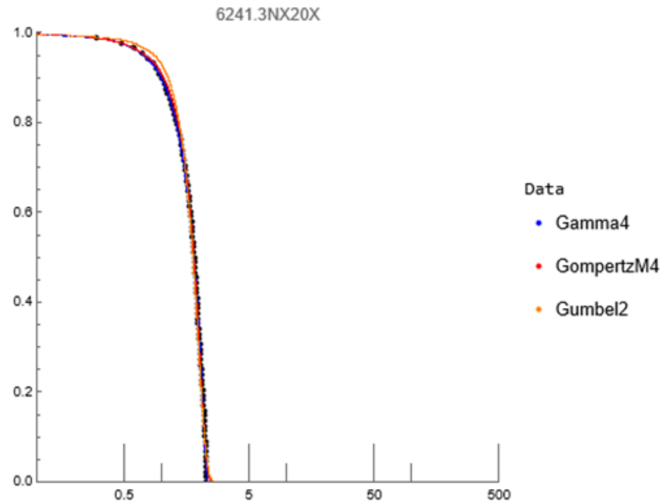
6241.3NX20X
1.0
0.8
0.6
0.4
0.2
0.0
0.5
5
50
500
Data
Gamma4
GompertzM4
Gumbel2

(a)

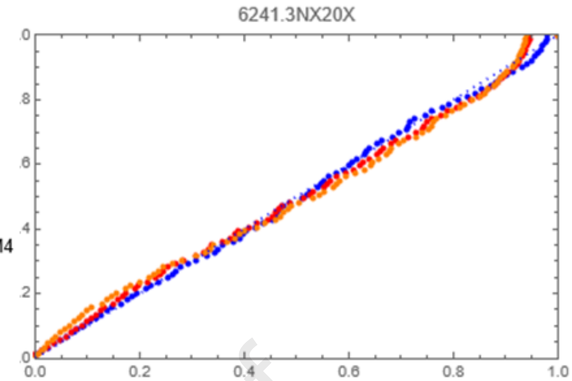
6241.3NX20X
0.0
0.2
0.4
0.6
0.8
1.0

(b)

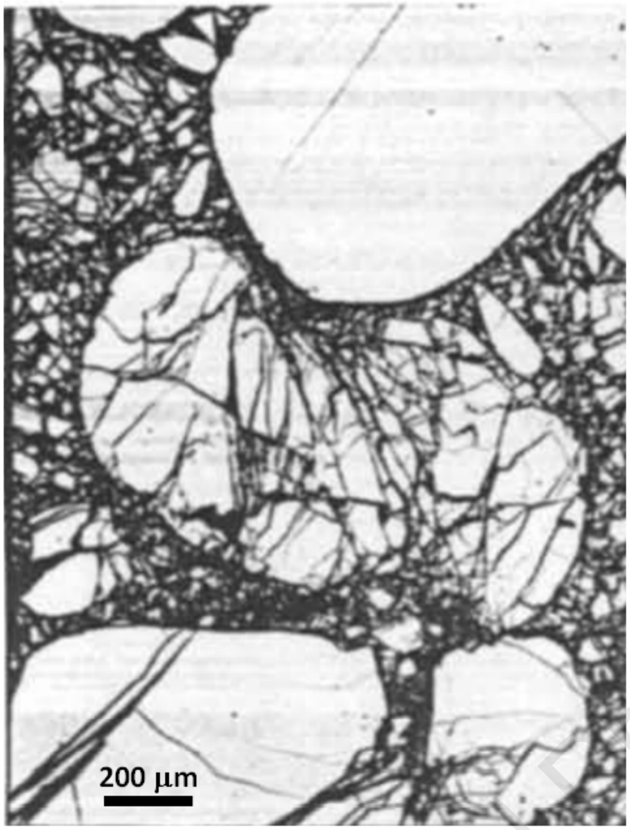

(a)

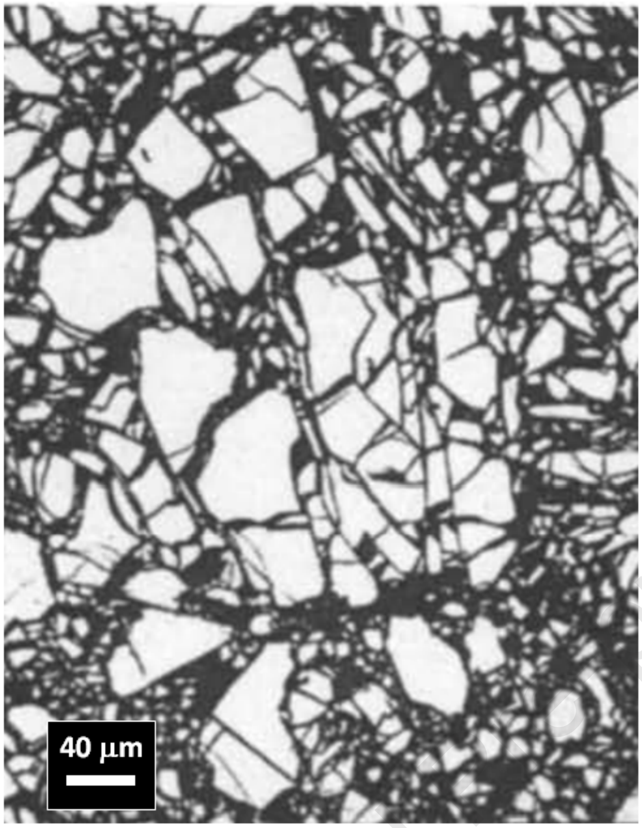

(b)

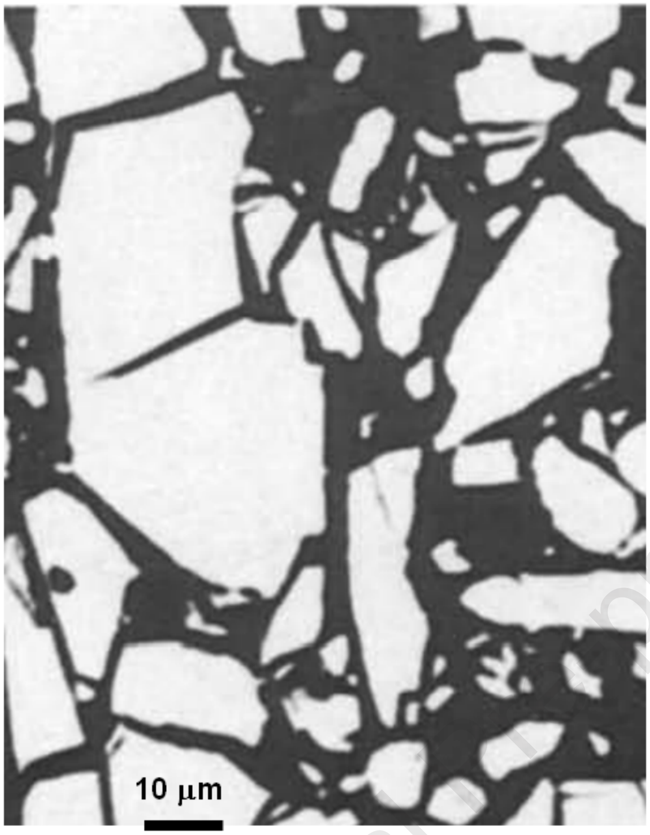

(c)

Highlights

- Cataclasite fragment size distributions are analysed.
- Power-law and log-normal distributions tend to be poor fits to these data.
- Best-fit Generalised Gamma distributions are consistent with theory.
- Best fit Extreme Value and Generalised Pareto distributions also are good fits.
- Linear and/or collisional fragmentation models provide similar results.